Molecular Therapy
Original Article

Efficient Non-viral Gene Delivery into Human Hematopoietic Stem Cells by Minicircle *Sleeping Beauty* Transposon Vectors

Marta Holstein,[1] Cristina Mesa-Nuñez,[2,3] Csaba Miskey,[1] Elena Almarza,[2,3] Valentina Poletti,[4,12] Marco Schmeer,[5] Esther Grueso,[1] Juan Carlos Ordóñez Flores,[1] Dennis Kobelt,[6] Wolfgang Walther,[6] Manish K. Aneja,[7] Johannes Geiger,[7] Halvard B. Bonig,[8] Zsuzsanna Izsvák,[9] Martin Schleef,[5] Carsten Rudolph,[7,10] Fulvio Mavilio,[4,11] Juan A. Bueren,[2,3] Guillermo Guenechea,[2,3] and Zoltán Ivics[1]

[1]Transposition and Genome Engineering, Division of Medical Biotechnology, Paul Ehrlich Institute, Langen, Germany; [2]Division of Hematopoietic Innovative Therapies, Centro de Investigaciones Energéticas Medioambientales y Tecnológicas and Centro de Investigación Biomédica en Red de Enfermedades Raras (CIEMAT/CIBERER), Madrid, Spain; [3]Advanced Therapies Unit, Instituto de Investigación Sanitaria Fundación Jiménez Díaz (IIS-FJD, UAM) Madrid, Spain; [4]Genethon, Evry, France; [5]PlasmidFactory GmbH & Co. KG, Bielefeld, Germany; [6]Translational Oncology, Experimental and Clinical Research Center, Charité University Medicine, Berlin, Germany; [7]ethris GmbH, Planegg, Germany; [8]Department of Transfusion Medicine and Immunohematology, Johann-Wolfgang-Goethe Universität, Frankfurt, Germany; [9]Mobile DNA, Max Delbrück Center for Molecular Medicine in the Helmholtz Association (MDC), Berlin, Germany; [10]Department of Pediatrics, Ludwig Maximilian University, Munich, Germany; [11]Department of Life Sciences, University of Modena and Reggio Emilia, Modena, Italy

The *Sleeping Beauty* (SB) transposon system is a non-viral gene delivery platform that combines simplicity, inexpensive manufacture, and favorable safety features in the context of human applications. However, efficient correction of hematopoietic stem and progenitor cells (HSPCs) with non-viral vector systems, including SB, demands further refinement of gene delivery techniques. We set out to improve SB gene transfer into hard-to-transfect human CD34$^+$ cells by vectorizing the SB system components in the form of minicircles that are devoid of plasmid backbone sequences and are, therefore, significantly reduced in size. As compared to conventional plasmids, delivery of the SB transposon system as minicircle DNA is ~20 times more efficient, and it is associated with up to a 50% reduction in cellular toxicity in human CD34$^+$ cells. Moreover, providing the SB transposase in the form of synthetic mRNA enabled us to further increase the efficacy and biosafety of stable gene delivery into hematopoietic progenitors *ex vivo*. Genome-wide insertion site profiling revealed a close-to-random distribution of SB transposon integrants, which is characteristically different from gammaretroviral and lentiviral integrations in HSPCs. Transplantation of gene-marked CD34$^+$ cells in immunodeficient mice resulted in long-term engraftment and hematopoietic reconstitution, which was most efficient when the SB transposase was supplied as mRNA and nucleofected cells were maintained for 4–8 days in culture before transplantation. Collectively, implementation of minicircle and mRNA technologies allowed us to further refine the SB transposon system in the context of HSPC gene delivery to ultimately meet clinical demands of an efficient and safe non-viral gene therapy protocol.

INTRODUCTION

Gene therapy of hematopoietic stem and progenitor cells (HSPCs) aims at the lifelong genetic correction of patients' blood progenitors, and it has been successfully applied in clinical settings to treat a variety of monogenic diseases, including primary immunodeficiencies.[1] Along with undisputed therapeutic benefits achieved after transplantation of genetically corrected autologous HSPCs, adverse events of the treatment have been observed in some clinical trials relying on gene delivery by gammaretroviral (γRV) vectors.[2–5] Although highly efficient in HSPC transduction, γRV vectors used in those trials unfortunately turned out to be genotoxic in the long term. The undesired insertional mutagenesis manifested in some of the patients by the development of leukemia, thereby raising serious safety concerns with the use of these vectors. As a consequence, substantial work has been dedicated to crafting advanced and safer vector systems, including self-inactivating (SIN)-γRV and SIN-lentiviral (SIN-LV) vectors devoid of enhancer/promoter sequences in their 3′ long terminal repeats (LTRs).[6–8] On the other hand, non-viral gene delivery by the *Sleeping Beauty* (SB) transposon system, with a close-to-random integration profile[9–13] and negligible transcriptional activities associated with the transposon-specific inverted terminal repeats (ITRs),[14] has been developed as an alternative to viral vectors commonly used

Received 28 February 2017; accepted 12 January 2018;
https://doi.org/10.1016/j.ymthe.2018.01.012.

[12]Present address: Dana-Farber Cancer Institute, Harvard Medical School, Boston, MA, USA

Correspondence: Zoltán Ivics, Paul Ehrlich Institute, Paul Ehrlich Str. 51-59, 63225 Langen, Germany.
E-mail: zoltan.ivics@pei.de

Please cite this article in press as: Holstein et al., Efficient Non-viral Gene Delivery into Human Hematopoietic Stem Cells by Minicircle *Sleeping Beauty* Transposon Vectors, Molecular Therapy (2018), https://doi.org/10.1016/j.ymthe.2018.01.012

in gene therapy trials. However, some technical challenges to the clinical implementation of the SB system have remained unmet.

The SB gene delivery technology is typically provided in the form of two plasmid DNA-based vectors: the first carrying a transposon unit defined by SB's ITRs that flank a gene of interest to be inserted into the genome, and the second encoding the SB transposase, the enzymatic component of the system. Upon its transient expression, the SB transposase recognizes and binds the ITRs and excises the transposon unit from the donor construct and integrates it into a genomic locus, thereby leading to persistent expression of the gene of interest in genetically modified cells and their progeny. Since its reactivation by means of reverse mutagenesis from fossil sequences found in fish genomes,[15] the activity of the SB transposon system has been significantly enhanced by molecular evolution, resulting in a superior, hyperactive variant of the SB transposase called SB100X.[16] This non-viral gene delivery tool has been successfully employed for versatile purposes of genome manipulation in animals (reviewed in Ivics et al.[17]), including functional cancer gene screens (also reviewed[18,19]), and germline gene transfer in experimental animals.[20–22] In gene therapy applications, the SB transposon system has been successfully adapted to render sustained expression of therapeutic transgenes for the treatment of a variety of animal disease models, following both *ex vivo* and *in vivo* gene delivery (reviewed elsewhere[23–26]). After promising preclinical validation, it finally entered the clinics in the context of cancer gene therapy aiming at redirecting T cell-mediated immune responses toward B cells malignancies.[27] Stable delivery of a CD19-specific chimeric antigen receptor (CAR) to T cells by applying this novel non-viral approach has been evaluated in ongoing human trials as efficacious and safe, and the manufacture of anti-tumor cell products of clinical grade has been assessed as cost effective and less laborious than that achieved by recombinant retroviral transduction.[13,28–30]

Implementation of the SB transposon system for gene therapy of the HSPC system is, however, hampered by a low efficiency of plasmid DNA delivery into stem cells in general.[16,31] Although it has been greatly improved by the use of nucleofection, an advanced technique of electroporation achieved by a combination of electrical pulses and cell type-specific solutions facilitating more efficient transfer of exogenous nucleic acids to both cytoplasm and nucleus,[32,33] non-viral gene delivery into HSPCs is still considered to be inefficient when compared with viral technologies. In addition, such a physical way of naked plasmid DNA delivery into HSPCs results in an excessive loss of cell viability, and the observed cytotoxicity increases proportionally to plasmid DNA load.[34] Moreover, unmethylated CG dinucleotide (CpG) motifs present in the bacterial backbone of conventional plasmid vectors have been postulated to trigger immunogenic responses against foreign DNA.[35–37] Finally, the presence of an antibiotic resistance gene typically present in plasmid vectors raises additional safety concerns in the context of gene therapy.

In efforts to address the limitations of non-viral gene transfer into HSPCs, we modified the conventional plasmid DNA-based form of the SB transposon system by employing the minicircle (MC) technology. MCs are supercoiled minimal expression cassettes developed for application in non-viral gene delivery. They are derived from their parental plasmids via an intramolecular recombination process, during which the majority of bacterial backbone sequences are depleted from the vector.[38–40] The MC vectors are, therefore, significantly reduced in size, and, as a consequence, they have been shown to enhance gene delivery into a variety of cell lines *in vitro*[38,41,42] and into the liver,[43,44] lungs,[45] muscles,[41,46] and tumors[42,46] *in vivo*. MCs have served as a more efficient and advanced non-viral delivery method for targeted genetic modification using zinc-finger nucleases,[47] generation of induced pluripotent stem cells,[48] in vaccination therapy to enhance HIV-specific immune responses,[49] and in blood-based cancer detection.[50] The improved potential of MC DNA-based delivery was also evidenced in a preclinical gene therapy for episomal treatment of mucopolysaccharidosis type I[44] and familial hypercholesterolemia.[51] A proof-of-concept study on the SB transposon system coupled with the MC DNA technology was performed in the HeLa cell line, and lipofection-based intracellular delivery of the improved version of the system resulted in robust SB transposition and transgene integration.[52] Finally, implementation of the MC technology has recently been shown to enable superior stable gene transfer efficiencies in human T cells for advanced CAR-T cell engineering with SB transposon vectors.[13]

In the present work, we generated the SB transposon system in the form of MC DNA of high purity, and we successfully validated its enhanced integrative properties in human HSPCs. Moreover, we further refined our non-viral gene delivery strategy by supplying the SB100X transposase as an mRNA, as nucleofection of HSPCs with mRNA was shown to cause only marginal loss of cell viability compared to nucleofection with plasmid DNA.[53] A concept of SB transposase-encoding mRNA to be efficiently co-delivered with an SB transposon unit to somatic cells was originally tested in a mammalian cell line *in vitro* and in mouse liver *in vivo*, using an early version of the SB transposase called SB11.[54,55] For the purpose of improved mRNA-based delivery of the hyperactive SB100X transposase into HSPCs, we adopted a novel technology of chemically modified mRNA characterized by enhanced stability and lower immunogenicity called Stabilized Non-Immunogenic Messenger RNA (SNIM.RNA).[56] To our knowledge, it is the first report investigating the performance of MC DNA and synthetic mRNA platforms in human HSPCs in the context of non-viral, SB transposon system-mediated genome modification for persistent transgene delivery, and as such it presents a significant advance for SB transposon technology for clinical blood stem cell gene therapy.

RESULTS

Increased Cell Viability after Nucleofection with Minicircle DNA and Minicircle DNA/SNIM.RNA Platforms for Intracellular Delivery of the *Sleeping Beauty* Transposon System

Nucleofection of HSPCs is associated with significantly reduced cell viability, which, in turn, affects the overall yield of genetically

Please cite this article in press as: Holstein et al., Efficient Non-viral Gene Delivery into Human Hematopoietic Stem Cells by Minicircle *Sleeping Beauty* Transposon Vectors, Molecular Therapy (2018), https://doi.org/10.1016/j.ymthe.2018.01.012

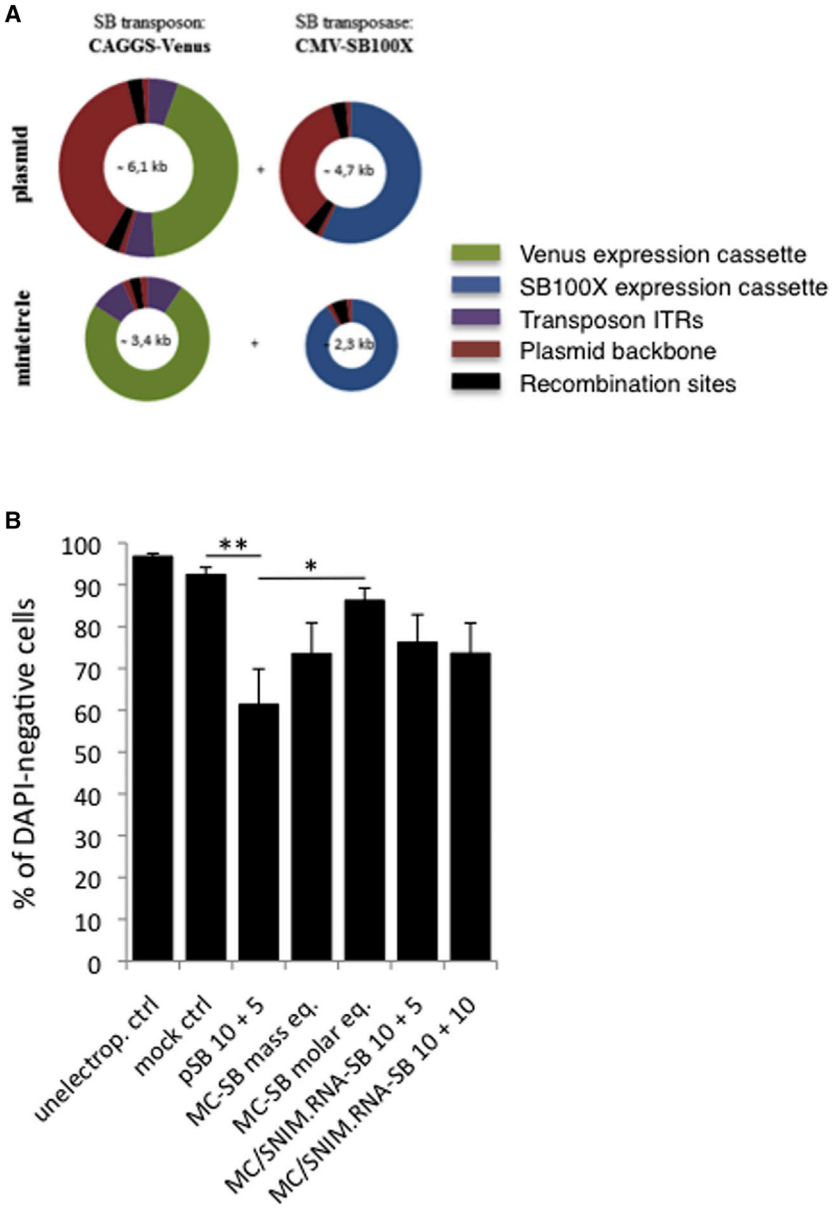

Figure 1. Minicircle-Based *Sleeping Beauty* Transposon Vectors and Cellular Toxicity of Gene Delivery 2 Days Post-nucleofection in CD34⁺ Cells

(A) MC vectors encoding the transposon or the transposase component of the SB system are derived from parental plasmids by intramolecular recombination. The parental transposon plasmid carries a CAGGS-Venus expression cassette (green) flanked by the ITRs of SB (purple), plasmid backbone sequences (red), and recombination sites (black). The parental transposase plasmid carries a CMV-SB100X expression cassette (blue), plasmid backbone sequences (red), and recombination sites (black). MCs have a markedly reduced size and lack most of the plasmid backbone sequences. (B) Percentage of DAPI-negative cells determined by flow cytometry. Data are expressed as means ± SEM (n = 5–6 per group). Asterisks indicate significant differences as determined by Student's t test (*$p < 0.05$ and **$p < 0.01$; 10 + 5 or 10 + 10 indicate the μg of the MC-Venus and the SB-transposase used during nucleofection).

modified cells. In our efforts to improve non-viral gene delivery into HSPCs for gene therapy purposes, we modified the conventional plasmid DNA form of the SB transposon system by applying MC DNA and SNIM.RNA technologies. The produced SB MCs were markedly reduced in their size compared to conventional plasmid DNA vectors, with 3.4 kb obtained for the MC-SB transposon (MC.T2-CAGGS-Venus) that carried a Venus reporter cassette and 2.3 kb for a CMV promoter-driven SB transposase (MC.SB100X) vector (Figure 1A; Figure S1).

We nucleofected human CD34⁺ cells with the MC.T2-CAGGS-Venus and MC.SB100X constructs, and we compared their performance with that of a conventional plasmid DNA form of the system. As a baseline condition, we opted for using 10 μg SB transposon and 5 μg SB transposase construct per 10^6 cells, as it was the optimal mass combination of both vectors in terms of overall efficiency of gene delivery and cytotoxicity (data not shown). To assess cellular toxicity, we implemented staining with DAPI followed by flow cytometry, by which the percentage of DAPI-negative and, thus, viable cell population was estimated at day 2 post-delivery.

As depicted in Figure 1B, a slight cellular toxicity was induced by nucleofection itself (mock control), but it was more pronounced when exogenous DNA was included in the reaction. Cell viability was compromised the most when the SB transposon system was introduced in the form of conventional plasmid DNA vectors, with only 61.3% ± 8.5% of DAPI-negative (i.e., live) cells detected within the total cell population. The highest cell viability (86.2% ± 3.0% of viable cells, a 1.4-fold increase) was observed after the delivery of MC DNA in amounts equimolar to the plasmid DNA-based SB transposon system. Equimass amounts of MC DNA vectors resulted in a 1.2-fold increase in the percentage of viable cells (73.5% ± 7.4%) compared to plasmid DNA, and this effect was maintained with SNIM.RNA encoding the SB100X transposase, with 76.2% ± 6.6% and 73.6% ± 7.3% of viable cells measured in the MC/SNIM.RNA-SB 10 + 5 and MC/SNIM.RNA-SB 10 + 10 conditions, respectively. Respective cellular toxicities associated with nucleic acid delivery by nucleofection were also assessed and confirmed by trypan blue (TB) staining and exclusion of dead cells following automated counting of unstained and, therefore, viable cells (data not shown). We conclude that excessive loss of HSPC viability is mostly related to the presence of plasmid DNA in the reaction and that this cellular toxicity can be

Please cite this article in press as: Holstein et al., Efficient Non-viral Gene Delivery into Human Hematopoietic Stem Cells by Minicircle *Sleeping Beauty* Transposon Vectors, Molecular Therapy (2018), https://doi.org/10.1016/j.ymthe.2018.01.012

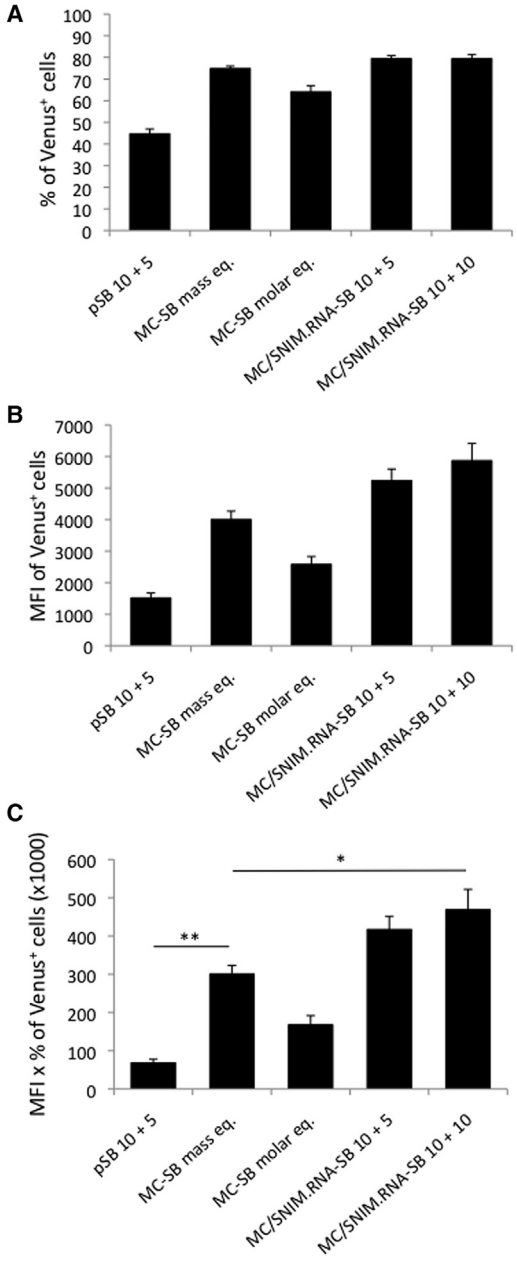

Figure 2. Efficiency of Transient Gene Expression following Minicircle-Based Delivery of *Sleeping Beauty* Transposon Vectors in CD34⁺ Cells

(A and B) The (A) percentage and (B) mean fluorescence intensity (MFI) of Venus⁺ cells determined by flow cytometry 2 days post-delivery. (C) Overall efficiency of transient gene delivery and expression calculated by multiplying the percentage of Venus⁺ cells and their MFIs. Data are expressed as means ± SEM (n = 5–6 per group). Asterisks indicate significant differences as determined by Student's t test (*$p < 0.05$ and **$p < 0.01$).

significantly reduced by implementing the MC DNA platform alone or in combination with SNIM.RNA technology for delivery of the SB transposon system.

Improved Intracellular Delivery of the *Sleeping Beauty* Transposon System by Minicircle Vectors into CD34⁺ Cells

High levels of genomic modification of hard-to-transfect HSPCs by means of a non-viral integrative technology necessitate efficient intracellular delivery of the implemented vector system. Vector size is a potent modulator of this parameter, and smaller constructs tend to cross the cell membrane and reach the nucleus more efficiently than larger ones.[57,58] In light of these facts, we implemented the MC DNA platform in order to significantly reduce SB transposon and transposase vectors in their size and, thus, enhance their rate of intracellular delivery, with a final goal of achieving sufficient levels of HSPC genome modification to be relevant for clinical gene therapy purposes. We examined the levels of intracellular delivery of SB vectors at day 2 post-nucleofection (transient gene delivery) by flow cytometry. The performance of the MC DNA platform alone or in combination with SNIM.RNA technology was compared with that of plasmid DNA in terms of percentage and mean fluorescence intensity (MFI) of Venus⁺ cells.

Whereas only 44.7% ± 2.2% of cells transiently expressing Venus could be obtained using standard plasmid DNA vectors, this value was markedly higher for the MC DNA platform, yielding overall transient gene delivery efficiencies of 74.9% ± 1.2% and 64.1% ± 2.9% in an equimass and equimolar comparison with the plasmid DNA system, respectively (Figure 2A). Moreover, improved transfection of MC vectors was also reflected by the MFI of Venus⁺ cells. Specifically, plasmid DNA was the least efficacious and led to MFI rates of only 1,516 ± 154 (Figure 2B). There were 2.6- and 1.7-fold increases in MFI values achieved in equimass (4,005 ± 264) and equimolar (2,581 ± 247) conditions, respectively. Interestingly, although the same type (MC DNA) and amount (10 μg) of the SB transposon vector was implemented in three different delivery variants (MC-SB mass equivalent, MC/SNIM.RNA-SB 10 + 5, and MC/SNIM.RNA-SB 10 + 10), slightly different MFI values were seen in those samples, with higher values obtained with SNIM RNA (MC/SNIM.RNA-SB 10 + 10, 5,870 ± 550; and MC/SNIM.RNA-SB 10 + 5, 5,239 ± 364). When the overall efficiency of transgene expression (percentages of Venus⁺ cells multiplied by their MFI values) was assessed, a very pronounced improvement was seen for both MC DNA only or for the MC DNA/SNIM.RNA combination (Figure 2C). More specifically, this value was 2.5-fold (167,931 ± 24,114) and 4.4-fold (300,531 ± 22,234) higher for MC DNA in an equimolar and equimass comparison with plasmid DNA (68,441 ± 9,463), respectively. Advantageous gene transfer promoted by MC DNA was even more striking in samples with SNIM.RNA implemented for SB100X transposase delivery, with 6.1-fold (417,189 ± 33,956) and 6.8-fold (468,790 ± 53,083) increases in relative transient gene delivery levels detected in the MC/SNIM.RNA-SB 10 + 5 and MC/SNIM.RNA-SB 10 + 10 samples, respectively. Taken together, the MC DNA platform alone or in combination with SNIM.RNA technology is capable of delivering the SB transposon system into HSPCs significantly more efficiently than conventional plasmids, suggesting that this improved platform would also result in enhanced efficacies of stable transposition.

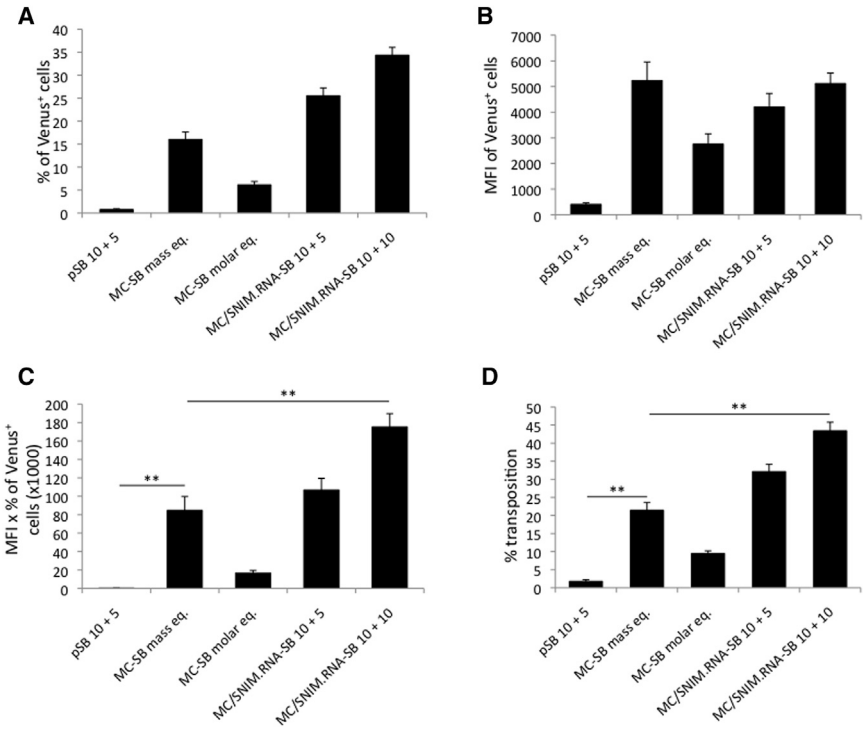

Figure 3. Long-Term Gene Expression following Minicircle-Based Delivery of *Sleeping Beauty* Transposon Vectors in CD34⁺ Cells

(A and B) The (A) percentage and (B) mean fluorescence intensity (MFI) of Venus⁺ cells determined by flow cytometry 15 days post-delivery. (C) Overall efficiency of gene expression calculated by multiplying the percentage of Venus⁺ cells and their MFIs. (D) Relative transposition efficiency determined by the percentage of Venus⁺ cells at day 2 post-nucleofection that retained Venus expression at day 15. Data are expressed as means ± SEM (n = 5–6 per group). Asterisks indicate significant differences as determined by Student's t test (*$p < 0.05$ and **$p < 0.01$).

Efficient Stable Delivery of the *Sleeping Beauty* Transposon System in the Form of a Minicircle DNA/SNIM.RNA Combination into CD34⁺ Cells

Our main goal behind implementing the MC DNA and SNIM.RNA technologies was to improve non-viral stable gene integration/expression in hard-to-transfect HSPCs. To evaluate vector performance in terms of SB-mediated genome modification, nucleofected CD34⁺ cells were maintained in culture for a prolonged period of time. In the absence of transposase, as expected, the initial (transient) levels of Venus reporter expression gradually diminished during cell expansion post-nucleofection, with plasmid and MC vectors most likely undergoing cellular degradation by cytosolic nucleases[59] and being successively excluded from cell cultures with each cell division. The slowly attenuated residual plasmid and MC DNA-specific transgene expression was, therefore, undetectable by flow cytometry beyond 14–19 days post-delivery (Figure S2). However, in the presence of transposase, following an initial decline until day 12 post-nucleofection, Venus expression was stably maintained thereafter for at least 62 days after nucleofection (end of experiment) (Figure S2), likely because the Venus signal was derived from genomically integrated transgenes.

The least efficient plasmid DNA-based delivery of the SB transposon system into CD34⁺ cells also resulted in very low numbers of Venus-expressing cells at day 15 post-nucleofection (only 0.8% ± 0.2% with an overall MFI of 405 ± 63; Figures 3A and 3B, respectively). In contrast, implementation of the MC vectors in equimolar amounts resulted in a significantly higher representation of Venus-expressing cells (6.1% ± 0.7%) carrying at least one copy of the SB transposon in their genomes (Figure 3A). Improved SB integration from MC vectors was accompanied by a 6.8-fold higher MFI of Venus signal (2,754 ± 403) (Figure 3B). As expected, in a mass-to-mass comparison of the two delivery platforms, the outperformance of MC DNA over conventional plasmids was even more apparent, giving rise to 16.0% ± 1.6% of Venus-expressing cells (Figure 3A) with an MFI of 5,231 ± 726 (Figure 3B). Finally, the most significant improvement in stable gene delivery could be achieved when the MC-based SB transposon was complemented with SNIM.RNA as a transient source of the SB100X transposase, with 25.5% ± 1.7% and 34.4% ± 1.7% of Venus⁺ cells (Figure 3A) with MFIs of 4,207 ± 523 and 5,117 ± 410 detected in the MC/SNIM.RNA-SB 10 + 5 and MC/SNIM.RNA-SB 10 + 10 samples, respectively (Figure 3B).

Similar to the analysis of transient gene expression (Figure 2), the overall efficiency of transgene expression at day 15 post-transfection (percentages of Venus⁺ cells multiplied by their MFI values) in expanded, CD34⁺ cell-derived populations revealed a dramatic outperformance of our dual MC DNA/SNIM.RNA delivery approach over conventional plasmid DNA vectors (Figure 3C). The calculated overall efficiency of transgene expression reached values of 106,793 ± 12,647 and 175,297 ± 14,299 in the case of MC/SNIM.RNA-SB 10 + 5 and MC/SNIM.RNA-SB 10 + 10 delivery variant, respectively (Figure 3C). The SB100X transposase provided in the form of MC DNA was in general less efficient than SNIM.RNA, with overall values of 84,680 ± 15,070 and 16,720 ± 2,810 determined for the mass and molar equivalents of the plasmid DNA platform, respectively. The MC vectors, however, were still far more efficient than plasmid DNA at supporting SB-mediated HSPC genome modification. The implementation of the SB transposon system in the form of conventional plasmid DNA yielded overall combined values of stable gene delivery into CD34⁺ cells of only 290 ± 69, which was ~600-fold less efficient than that achieved in our best condition (MC/SNIM.RNA-SB 10 + 10) (Figure 3C).

Please cite this article in press as: Holstein et al., Efficient Non-viral Gene Delivery into Human Hematopoietic Stem Cells by Minicircle *Sleeping Beauty* Transposon Vectors, Molecular Therapy (2018), https://doi.org/10.1016/j.ymthe.2018.01.012

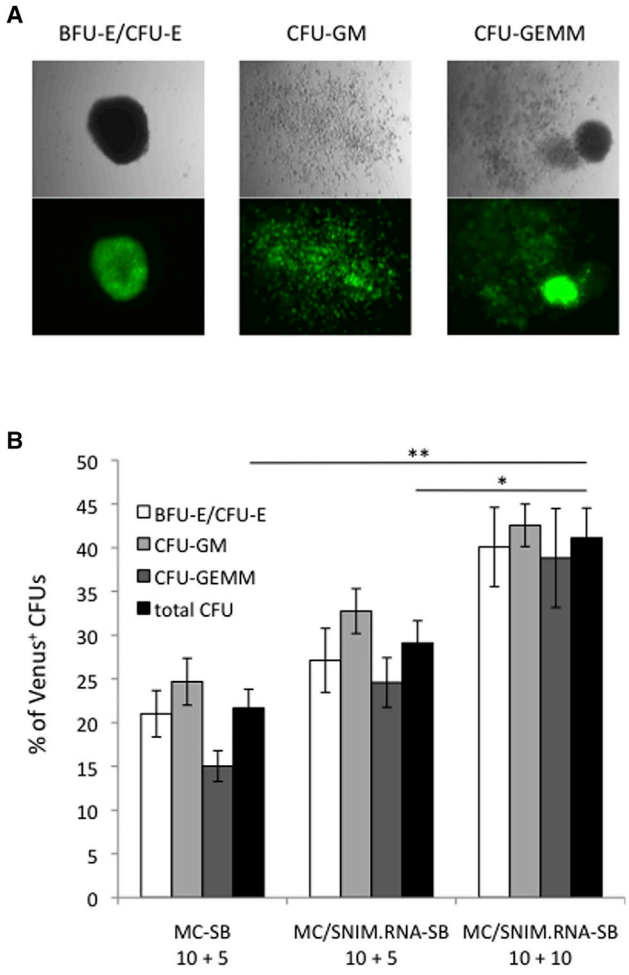

Figure 4. Stable Gene Transfer and Expression Mediated by *Sleeping Beauty* Transposons in Committed Hematopoietic Progenitor Cells

(A) Representative images of colonies generated after culture of nucleofected cells in methylcellulose medium enriched with a cytokine cocktail supporting the formation of burst-forming unit-erythroid (BFU-E), colony-forming unit-erythroid (CFU-E), colony-forming unit-granulocyte, macrophage (CFU-GM), and colony-forming unit-granulocyte, erythroid, macrophage, megakaryocyte (CFU-GEMM). (B) Percentage of colonies stably expressing Venus after MC DNA only and MC DNA/SNIM.RNA-based delivery of the SB transposon system. Data are expressed as means ± SEM (n = 3 per group). Asterisks indicate significant differences as determined by Student's t test (*$p < 0.05$ and **$p < 0.01$).

Another way of assessing the efficiency of the SB transposon system for stable gene delivery is to calculate the fraction of cells that were initially Venus$^+$ at day 2 post-transfection that retained Venus expression after prolonged cell expansion (i.e., at day 15, when almost no Venus expression was observed in cells transfected without the transposase; Figure S2). The MC DNA platform was associated with significantly higher levels of stable gene transfer when compared to conventional plasmid DNA, with 21.4% ± 2.2% and 9.5% ± 0.7% of cells retaining the Venus signal in equimass and equimolar conditions, respectively (Figure 3D). In contrast, only 1.8% ± 0.5% of the initially Venus$^+$ cell fraction underwent transposition after plasmid DNA-based delivery of the SB transposon system and expressed Venus at day 15 post-nucleofection. The SB100X transposase provided in the form of SNIM.RNA supported the highest level of stable transgene expression at 32.1% ± 2.0% and 43.4% ± 2.4% in the MC/SNIM.RNA-SB 10 + 5 and MC/SNIM.RNA-SB 10 + 10 conditions, respectively, highlighting the advantage of our dual MC/SNIM.RNA-SB delivery approach (Figure 3D).

Sleeping Beauty-Mediated Genetic Modification of CD34$^+$ Cells Is Not Restricted to Specific Committed Progenitors

To assess whether stable genetic modification mediated by nucleofection with the different SB platforms was restricted to specific hematopoietic progenitor cells, we performed colony-forming unit-culture (CFU-C) assays *in vitro* (Figure 4A) using our three best delivery variants, namely MC-SB 10 + 5, MC/SNIM.RNA-SB 10 + 5, and MC/SNIM.RNA-SB 10 + 10.

In each of three independently performed CFU-C assays, the presence of Venus$^+$ cells could be demonstrated in burst- and colony-forming units of erythroid cell type (BFU-E/CFU-E), colony-forming units with granulocytes and macrophages (CFU-GM), and mixed colony-forming units of myeloid and erythroid type (CFU-GEMM) following MC DNA- and MC DNA/SNIM.RNA-based delivery of the SB transposon system. Although no apparent differences were seen in the overall CFU potential of the cells following nucleofection with the three different delivery variants (Figure S3), differences were clearly visible with regard to the contribution of Venus$^+$ CFUs to the total CFU counts (Figure 4B). As previously seen in liquid cultures, the SB transposon system in the form of MC DNA (equimass condition, MC-SB 10 + 5) was associated with the lowest efficiency to generate Venus$^+$ colonies (21.7% ± 2.2% of CFUs with detectable long-term Venus expression, including 21.0% ± 2.7%, 24.7% ± 2.7%, and 15.0% ± 1.8% of Venus$^+$ BFU-E/CFU-E, CFU-GM, and CFU-GEMM, respectively). The MC/SNIM.RNA platform was more efficient at supporting SB transposition, which resulted in 29.1% ± 2.5% of Venus-expressing CFUs in the MC/SNIM.RNA 10 + 5 sample. In detail, there was a 1.3 (27.1% ± 3.7%), 1.3 (32.7% ± 2.6%), and 1.6 (24.6% ± 2.8%) times more frequent appearance of SB-modified colonies of erythroid (BFU-E/CFU-E), granulocyte/macrophage (CFU-GM), and mixed (CFU-GEMM) type, respectively, observed in this sample when compared to the MC-SB 10 + 5 condition. Similar to the results obtained after flow cytometry-based analysis of stable gene delivery, the MC/SNIM.RNA-SB 10 + 10 combination of the SB transposon system appeared to be the most efficient at genomic modification of hematopoietic progenitors, and it yielded on average 41.1% ± 3.4% of Venus-expressing colonies (a 1.9-fold increase compared to the MC-SB 10 + 5 condition), with 40.1% ± 4.5%, 42.6% ± 2.4%, and 38.8% ± 5.7% of BFU-E/CFU-E, CFU-GM, and CFU-GEMM, respectively, bearing the Venus signal. In aggregate, HSPC genome manipulation by the SB transposon system, and most significantly with the MC DNA/SNIM.RNA vector combination, yields highly efficient transgene expression in committed progenitor cells of the erythroid and myeloid lineages.

Please cite this article in press as: Holstein et al., Efficient Non-viral Gene Delivery into Human Hematopoietic Stem Cells by Minicircle *Sleeping Beauty* Transposon Vectors, Molecular Therapy (2018), https://doi.org/10.1016/j.ymthe.2018.01.012

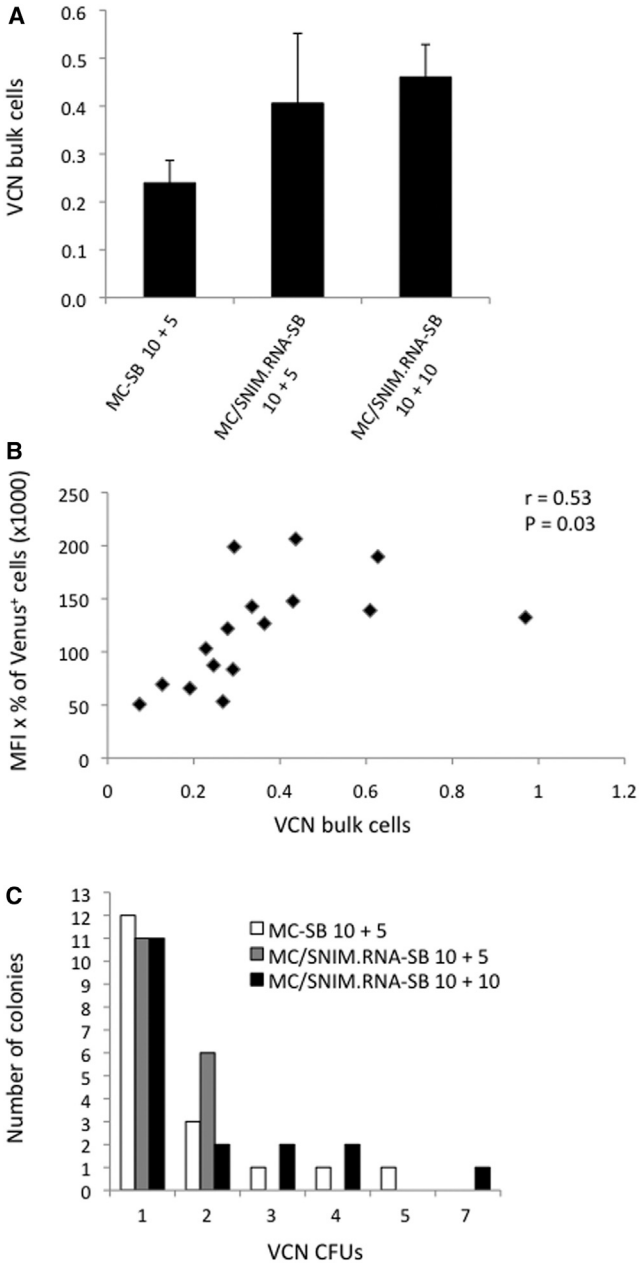

Figure 5. Vector Copy Numbers in *Sleeping Beauty*-Engineered CD34$^+$ Cells
(A) Determination of vector copy number (VCN) in bulk cells cultured for 3 weeks in liquid culture. Data are expressed as means ± SEM (n = 5–6 per group). (B) Correlation between VCN determined in bulk cells and relative stable gene delivery efficiency defined as percentage Venus$^+$ cells multiplied with their MFIs. (C) VCN determined in CFUs. r, Pearson coefficient of the correlation; p, significance coefficient.

The Minicircle DNA and Minicircle DNA/SNIM.RNA-SB Gene Delivery Platforms Enable Efficient Transgene Integration in CD34$^+$ Cells

Next, we were interested in the numbers of SB transposon integrations obtained per HSPC genome, another parameter reflecting the efficiency of persistent gene delivery. qPCR was performed using unselected bulk cell populations (containing both Venus$^+$ and Venus$^-$ cells) harvested 3 weeks post-nucleofection. For these analyses, three of our best and, therefore, most relevant delivery variants, MC-SB 10 + 5, MC/SNIM.RNA-SB 10 + 5, and MC/SNIM.RNA-SB 10 + 10, were chosen.

The average vector copy number (VCN) per diploid genome was 0.24 ± 0.05 in the MC-SB 10 + 5 condition (Figure 5A). With SNIM.RNA, 0.41 ± 0.15 and 0.46 ± 0.07 copies of the integrated transposon per cell were detected upon MC/SNIM.RNA-SB 10 + 5 and MC/SNIM.RNA-SB 10 + 10 delivery, respectively. The tendency toward higher VCNs is, thus, associated with the higher efficiency of stable gene transfer observed in both DNA/SNIM.RNA-SB delivery variants. Indeed, as shown in Figure 5B, there was a significant correlation between the obtained VCNs/genome and the relative efficiency of stable gene delivery (as defined by multiplying percent Venus$^+$ cells by their MFIs at day 15 post-delivery).

To restrict the analysis to only those cells in which transposition definitely took place, individual Venus$^+$ CFUs generated in methylcellulose medium were picked, and genomic DNA was isolated and subjected to droplet digital PCR. This qPCR analysis allowed us to precisely determine the number of integrated vector copies at the cell clonal level despite very limited amounts of DNA present in the reaction. These analyses revealed that 64% of the analyzed colonies carried 1 copy of the Venus transgene in the genome, regardless of the vector combination applied to deliver the SB transposon system (Figure 5C). More specifically for the MC-SB 10 + 5 delivery variant, 12 of 18 colonies harbored 1 copy of the SB transposon per diploid genome. Two copies could be found in 3 independent colonies, and colonies with 3, 4, and 5 copies were each represented only once. In the MC/SNIM.RNA-SB 10 + 5 delivery variant, the obtained VCN/genome was more homogeneous; the absence of colonies with VCN/genome >2 correlated with slightly lower MFI values recovered in this delivery variant (Figure 3B). The most effective delivery form of the SB transposon system (MC/SNIM.RNA-SB 10 + 10) gave rise to 11 colonies of 18 analyzed with a single-copy transposon integration, 6 colonies containing 2–4 copies/genome, and a single colony with up to 7 copies of the Venus cassette per genome (Figure 5C).

In sum, quantitative analysis of VCNs in bulk cell populations and in individual colonies complements the data on stable gene expression determined by flow cytometry and clonogenic assays. Importantly, these analyses show that highly efficient gene delivery by the MC platform, either alone or in combination with the SNIM.RNA technology, is not accompanied by excessive copy numbers of integrated transgenes per genome.

Random Profile of *Sleeping Beauty*-Mediated Transgene Integration in CD34$^+$ Cells

Non-targeted insertions of therapeutic foreign DNA into the genome are subject to position effects, which may alter cell physiology and lead to malignant transformations. To assess the biosafety of the SB

Please cite this article in press as: Holstein et al., Efficient Non-viral Gene Delivery into Human Hematopoietic Stem Cells by Minicircle *Sleeping Beauty* Transposon Vectors, Molecular Therapy (2018), https://doi.org/10.1016/j.ymthe.2018.01.012

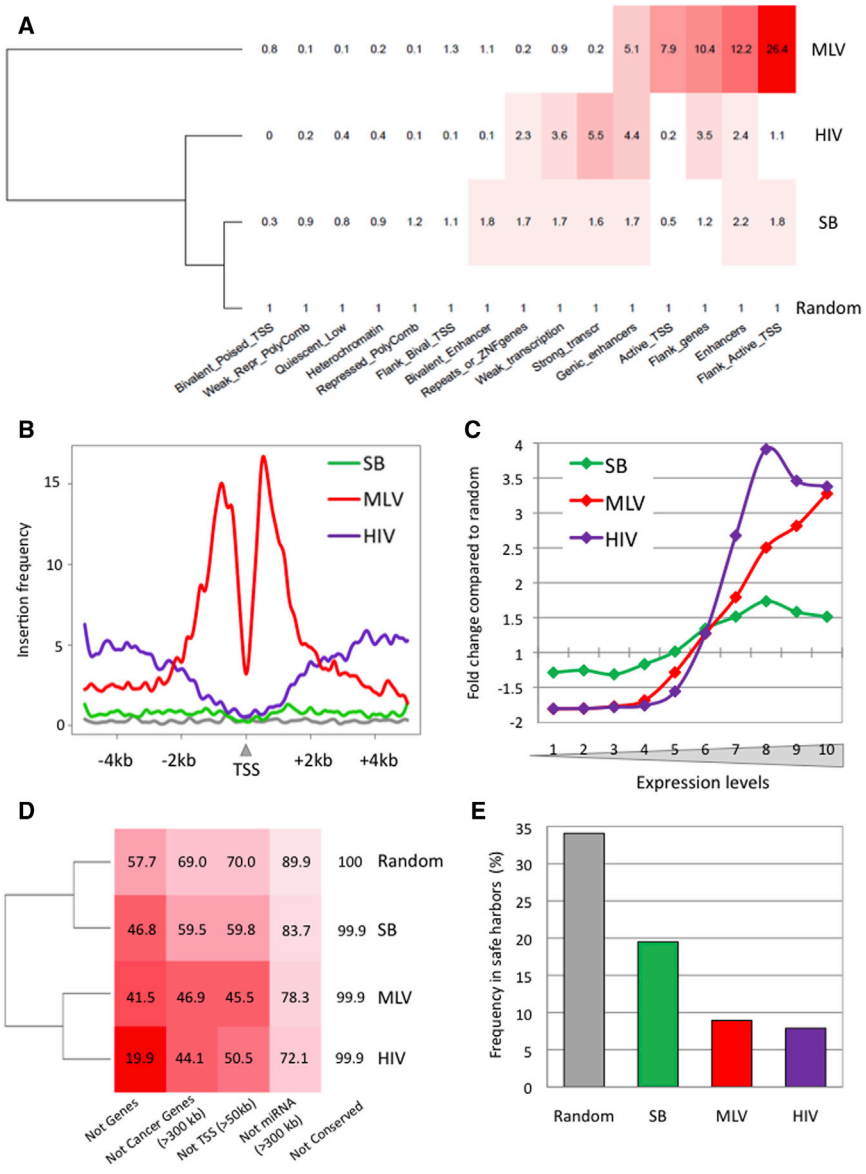

Figure 6. Genome-wide Distribution of *Sleeping Beauty* Transposon, MLV-Derived Gammaretroviral, and HIV-1-Derived Lentiviral Integrations in CD34⁺ Cells

(A) Distribution of MLV, HIV, and SB insertions in functional genomic segments of human G-CSF-mobilized HSPCs. Numbers show relative enrichment above the random frequency (set to 1). Color intensities depict the degree of deviation from the expected random distribution. The cladogram was drawn on the basis of row means. (B) Distribution of vector insertion sites around transcriptional start sites (TSSs). The gray line corresponds to random insertion frequency. (C) Correlation between integration rates and transcriptional activity of the insertion sites. The numbers of the x axis stand for groups of transcription units of increasing activity in human HSPCs. Negative and positive values of the y axis indicate under- and over-representation in fold change over the random expected insertion frequency, shown as 1. (D) Representation of vector insertion sites cosrresponding to genomic safe harbor criteria. The numbers represent percent values of all insertions of the corresponding group. Color intensities imply deviation from an ideal 100% representation. (E) Overall representation of insertion sites in genomic safe harbors.

vector system, we performed a genome-wide insertion site profiling of SB integrations in human hematopoietic progenitors after MC DNA and MC DNA/SNIM.RNA-based delivery by massively parallel sequencing. PCR-based insertion site libraries were generated from genomic DNA isolated from CD34$^+$ cells at least 3 weeks post-nucleofection. The bioinformatic analysis using conservative filtering resulted in 875 and 14,127 unique insertion sites derived from the MC DNA and MC DNA/SNIM.RNA delivery methods, respectively. Since the difference of the transposase source in the two experimental conditions was of delivery method (DNA versus RNA) and not of type (amino acid composition), the two insertion site sets were united into a single pool for the downstream analysis. Then, we compared the SB integration profile with published or *ad hoc*-generated datasets of 32,574 γRV[60] and 58,294 HIV-derived lentiviral vector integration sites in human cord blood-derived HSPCs, using a computationally generated random integration dataset as a control.

At the DNA sequence level, TA dinucleotides positioned at the center of an 8-bp palindromic AT repeat, a canonical molecular signature of SB chromosomal integration,[9] were found as highly preferred sites of SB integration (Figure S4). Next, we profiled the SB insertions in functional genomic segments. These are regions of co-occurring epigenetic signal patterns, which were clustered together computationally, to comprise various functional partitions of the human genome.[61] We used 15- and 25-state chromatin models of granulocyte colony-stimulating factor (G-CSF)-mobilized primary HSPCs to compare the SB insertion profile to the distribution of murine leukemia virus (MLV)-derived γRV and HIV-derived lentiviral insertions in the human genome (Figure 6A; Figure S5). In agreement with earlier findings, we found that, while MLV and HIV insertions accumulated in loci flanking transcriptional start sites (TSSs) and within actively transcribed genes, respectively, SB insertions showed only a minor bias toward these genomic segments. Moreover, of the three studied gene vector systems, the overall profile of SB is the closest to a random distribution.

Next, we aimed at comparing the propensity of gene vectors to interact with host transcription by studying the integration frequency

Please cite this article in press as: Holstein et al., Efficient Non-viral Gene Delivery into Human Hematopoietic Stem Cells by Minicircle *Sleeping Beauty* Transposon Vectors, Molecular Therapy (2018), https://doi.org/10.1016/j.ymthe.2018.01.012

of MLV, HIV, and SB around TSSs and within transcription units of human HSPCs (Figures 6B and 6C). We found that, while MLV insertions peaked within a 4-kb window centered on TSSs, HIV had an integration bias away from the TSSs both to the upstream and toward the bodies of genes. On the contrary, the frequency of SB integrants in these segments was close to a distribution expected by random chance (Figure 6B). When the insertion frequencies in transcription units were related to the transcriptional activity at the insertion sites, we found that, although all the vectors showed a tendency to integrate into actively transcribed chromatin, SB insertions showed the least deviation from the random insertion rates both within silent and in highly expressed genes (Figure 6C). Moreover, in agreement with the tendency of the HIV and MLV to integrate within and in the upstream proximity of expressed genes, we found that the viral vectors had a larger propensity to hit genomic regions associated with human hematopoietic disorders than SB transposon vectors (Figure S6).

Integration of therapeutic gene constructs into genomic safe harbors (GSHs) in the human genome would prevent insertional mutagenesis and the associated risks of oncogenesis in gene therapy. GSHs are regions of the human genome that support predictable expression of newly integrated DNA without adverse effects on the host cell. GSHs can be bioinformatically allocated to chromosomal sites or regions if they satisfy the following criteria: (1) no overlap with transcription units, (2) at least 300-kb distance to cancer-related genes and (3) microRNA genes, and (4) at least 50-kb distance from TSSs of genes and (5) regions outside of ultraconserved regions.[62,63] Since transcription units can extend to long chromosomal territories, a hypothetical gene vector even with completely random insertion site distribution would integrate the transgene outside of genes with only ~58% probability (Figure 6D). We found that the biases of the MLV and HIV integration machinery toward expressed genes decreased the fraction of non-genic viral insertions to 41% and 20%, respectively. On the contrary, approximately 47% of all SB insertions were found outside of genes in HSPCs. Figure 6D also depicts that the insertion profile of SB segregates away from the insertion distribution of MLV and HIV and had a close-to-random pattern. In line with these observations, studying the insertion frequencies in the intersection of all five GSH criteria showed that SB has the safest expected insertion distribution of the tested vectors in a therapeutic context (Figure 6E). Collectively, our analysis on vector biosafety predicts a safer, thus favorable transgene insertion profile for SB over MLV- and HIV-based vectors in therapeutic gene transfer in human HSPCs.

Improved SB Gene Delivery Platforms Enable Efficient *In Vivo* Transgene Expression in Human Hematopoietic Cells Repopulating Immunodeficient Mice

Next we addressed the ability of the newly developed, MC-based SB gene delivery platforms to genetically modify human hematopoietic repopulating cells capable of conferring *in vivo* expression after transplantation into immunodeficient mice. Due to the toxicity (Figure 1) and relatively low efficiency of stable gene transfer (Figure 3) associated with the use of plasmid DNA *in vitro*, only the MC constructs were considered in these experiments. After nucleofection, cells were maintained for either 1–2.5 days (black dots) or 4–8 days (white dots) *in vitro* (Figure 7), with the purpose of minimizing potential homing defects associated with cell nucleofection. Thereafter, numbers equivalent to $0.7–1 \times 10^6$ nucleofected cells were transplanted into NOD-scid IL2Rg^{null} (NSG) mice irradiated with 1.5 Gy, as described in Materials and Methods.

As shown in Figure 7A, when recipients were transplanted with control CD34$^+$ cells, either not nucleofected (black and white dots) or nucleofected without DNA (gray dots), donor engraftment levels higher than 10% were observed in all instances (mean level of hCD45$^+$ cells: 37.8%). On the contrary, when cells were nucleofected with SB MCs and the transposase (either used as MC DNA or mRNA), a significant number of NSG recipients showed graft failure (levels of hCD45$^+$ cells: <1%). This was most evident when nucleofected cells were incubated for only 1–2.5 days (9 of 22 recipients failed to engraft human CD45$^+$ cells; black dots) compared to samples incubated for 4–8 days (11 of 12 recipients showed evident engraftment with hCD45$^+$ cells; white dots). Strikingly, when CD34$^+$ cells were nucleofected with the MC transposon plus the transposase mRNA and then maintained for 4–8 days in culture, all transplanted mice showed evident hematopoietic reconstitution, which resulted in engraftment levels very similar to those observed in mice transplanted with control CD34$^+$ cells (44.8% and 37.8%, respectively; $p < 0.05$).

Our results also demonstrated the expression of the Venus transgene in human hematopoietic cells engrafting the NSG mice (Figure 7B). Although the presence of Venus$^+$ cells was observed in all groups of transplanted mice, the infusion of nucleofected cells that were pre-incubated for 4–8 days facilitated the expression of the marker in every transplanted mouse (mean percentage of hCD45$^+$ cells positive for Venus expression: 13.44% and 13.42% in the MC-SB and the MC/SNIM.RNA-SB groups, respectively; $p < 0.05$).

To confirm that the expression of the Venus marker gene was not restricted to specific human hematopoietic lineages, the presence of Venus$^+$ cells was investigated in myeloid and lymphoid cells engrafting the bone marrow (BM) of transplanted NSG mice (see data in Figure 7C and representative analyses in Figure S7). Data in Figure 7C clearly demonstrate the presence of Venus$^+$ cells in both the human myeloid (CD33$^+$) and the lymphoid (CD19$^+$) cells. Even more, our data clearly show the presence of CD34$^+$ cells that expressed the marker gene, demonstrating transposition in primitive human hematopoietic repopulating cells that facilitated the *in vivo* expression of the transgene in engrafted cells. Consistent with overall engraftment levels (Figure 7A) and Venus expression (Figure 7B), the infusion of CD34$^+$ cells that had been nucleofected with MC-SB plus transposase mRNA and pre-incubated for 4–8 days resulted in the most consistent results of gene expression in all tested human hematopoietic lineages. Although differences in the proportion of Venus$^+$ cells could not be established between the different groups of transplanted mice, the presence of Venus$^+$ cells could be

Please cite this article in press as: Holstein et al., Efficient Non-viral Gene Delivery into Human Hematopoietic Stem Cells by Minicircle *Sleeping Beauty* Transposon Vectors, Molecular Therapy (2018), https://doi.org/10.1016/j.ymthe.2018.01.012

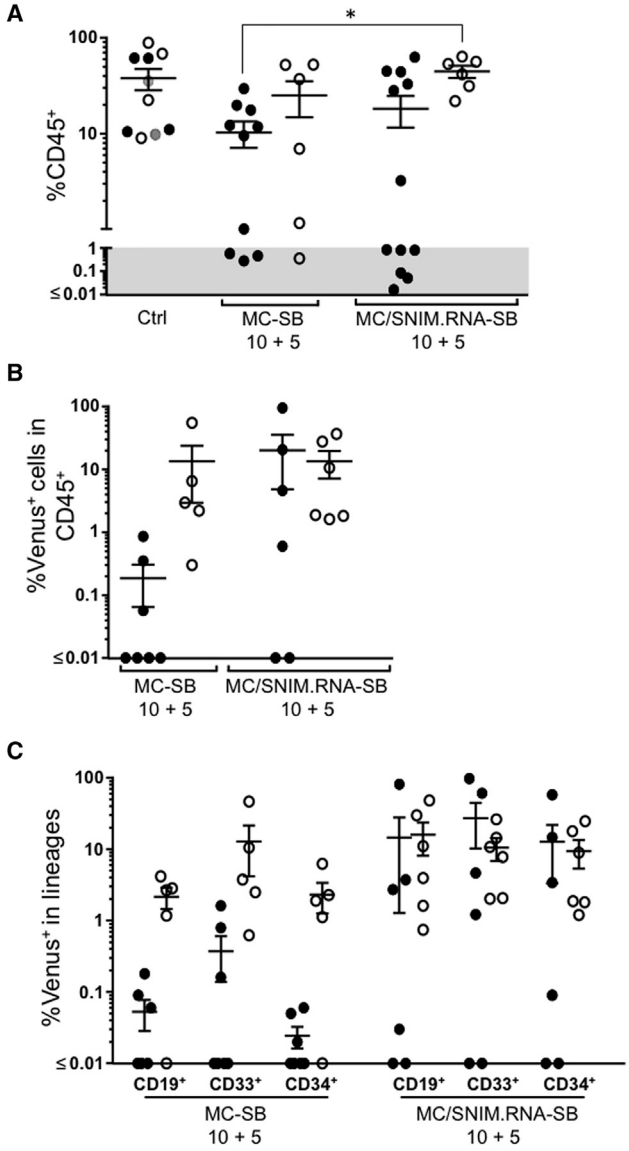

Figure 7. Analysis of Engraftment and Gene Expression in NSG Immunodeficient Mice Transplanted with Human CD34⁺ Cells Nucleofected with Different *Sleeping Beauty* Vector Components

(A) Analysis of human hematopoietic engraftment determined by the proportion of human CD45⁺ cells in the bone marrow of NSG mice transplanted with control CD34⁺ cells (Ctrl, not nucleofected, black and white dots or nucleofected without DNA, gray dots), or with CD34⁺ cells nucleofected with two different SB vector component combinations: MC/SB (10 μg Venus MC transposon + 5 μg MC SB transposase) and MC/SNIM.RNA-SB (10 μg Venus MC transposon + 5 μg RNA SB transposase). Black dots correspond to cells maintained for 1–2.5 days in culture before transplantation, whereas white dots correspond to incubations for 4–8 days. Gray dots correspond to nucleofected cells without DNA and incubated for 1–2.5 days. The gray area represents the limit considered for positive engraftment. In all instances, mice were analyzed at 3–4 months post-infusion. (B) Analysis of the percentage of Venus-expressing cells in human hematopoietic cells (CD45⁺) corresponding to animals repopulated with human cells (≥1% CD45⁺ cells in the BM of mice shown in (A). (C) Percentage of Venus⁺ cells in the myeloid (CD33⁺) and lymphoid (CD19⁺) population, as well as in hematopoietic progenitors (CD34⁺) corresponding to animals shown in (B). Data are expressed as mean ± SEM. Asterisks indicate significant differences as determined by Student's t test (*$p < 0.05$). Each dot represents data obtained from a single NSG-transplanted recipient. Data from 5 independent experiments are shown.

demonstrated in every single transplanted mouse in this particular experimental group.

DISCUSSION

Owing to their simplicity and inexpensive manufacture, plasmid DNA vectors remain a common delivery form of the non-viral SB transposon system in well-transfectable cell types. However, intracellular delivery of plasmid DNA vectors tends to be inefficient and toxic in some primary cell types, including HSPCs, which compromises the overall rates of SB-mediated genome modification. In the present study, we improved stable gene transfer by SB into human HSPCs.

In our first attempts toward enhancing the delivery and integrative activity of the SB transposon system in HSPCs, we modified conventional SB transposon and transposase plasmid vectors by employing the MC technology. It allowed us to significantly reduce both SB vectors in size by removing most of the bacterial backbone sequences from their parental plasmids. The presence of bacterial backbone elements is mandatory for vector propagation in *E. coli*, but it is completely redundant or even undesired for clinical applications.

The first evident advantage of using MC vectors over plasmids was related to increased cell survival rates following nucleofection of CD34⁺ cells (Figure 1). In a molar-to-molar comparison of both platforms, this might be partially explained by a mere reduction of the total DNA mass due to depletion of bacterial backbone sequences in both SB MC vectors. However, increased cell viability was also observed in a weight-to-weight comparison of both delivery platforms, pointing at intrinsic properties of plasmid DNA itself that possibly induce additional cytotoxicity *in vitro*. Unmethylated CpG motifs, which are highly enriched in the bacterial backbone of exogenously delivered plasmids, were shown to trigger strong inflammatory responses through Toll-like receptor-9[35,36] and/or interferon induction.[37] Activation of these cellular sensors might be a conceivable explanation for the observed nucleofection cytotoxicity and, thus, the exclusion of a large fraction of plasmid DNA-nucleofected cells from the rest of the proliferating HSPC culture. Indeed, removal of CpG motifs from plasmid DNA vectors was demonstrated to reduce inflammatory responses upon pulmonary gene delivery,[64] and vector CpG methylation was able to lower immune responsiveness toward non-self DNA and led to delayed clearance of transfected cells *in vivo*.[65]

Along with decreased levels of cytotoxicity, nucleofection of HSPCs with SB transposon components supplied as MCs resulted in enhanced transient gene delivery and more efficient stable genome modification as compared to conventional plasmid vectors (Figures 2, 3, and 5). The ultimate success of SB-mediated HSPC genome modification depends on several parameters, including the efficacy

Please cite this article in press as: Holstein et al., Efficient Non-viral Gene Delivery into Human Hematopoietic Stem Cells by Minicircle *Sleeping Beauty* Transposon Vectors, Molecular Therapy (2018), https://doi.org/10.1016/j.ymthe.2018.01.012

of cellular entry of the vector, nuclear localization of vector components, the levels of transposase expression, and, finally, transposon excision and integration activity in the nucleus. Although it is difficult to conclude at which of these gene transfer checkpoints the MC technology provides the most significant advantage, certain assumptions can be made. First, it has been speculated that, due to their smaller size, MC vectors cross cellular membranes more efficiently than plasmids.[38,41] In electroporation-mediated gene delivery, this would then be associated with better penetration of MC constructs through the pores of electro-permeabilized cell membranes.[41] Indeed, we observed an enrichment of Venus$^+$ cells at day 2 post-nucleofection of MC vectors (Figure 2A). Second, MC vectors may support enhanced transcription of transgene cassettes. Indeed, enhanced and sustained transgene expression has been seen in episomal gene therapy applications with MC vectors, with concomitant gene silencing commencing rapidly after hydrodynamic injection of parental plasmid vectors *in vivo*.[43,44] Covalent linkage of bacterial DNA sequences to a eukaryotic expression cassette has been suggested to facilitate the spreading of repressive chromatin formed primarily on the bacterial backbone, leading in turn to rapid loss of transgene expression from plasmid DNA vectors.[66,67]

Importantly, the MC platform led not only to more efficient transient gene delivery of the SB transposon system but also to greatly improved SB transposition rates (i.e., stable transgene integration) into the HSPC genome (Figure 3). The elevated levels of transposition observed in MC-SB samples are likely supported, at least in part, by the relatively short, 218-bp distance between the SB transposon ends in the MC-based transposon vector, owing to the depletion of the bacterial plasmid backbone. Indeed, SB transposition was shown to be far more efficient when the length of DNA sequence outside the transposon unit was shortened, likely by aiding transposon/transposase complex formation.[68]

In our efforts toward refinement of the SB transposon system for stable, non-viral gene transfer into HSPCs, we were able to further increase the rates of transposition by complementing MC-SB transposons with an mRNA source of the SB100X transposase (Figures 1, 2, 3, 4, and 5). By exploiting the mRNA approach for intracellular delivery, additional hurdles of gene transfer typical for DNA-based vectors can be avoided. For example, upon application of an electric pulse, mRNA translocates into the cytoplasm and is then readily available for the host translational machinery and protein production. In our approach for stable gene delivery into HSPCs, we utilized the hyperactive SB100X transposase and the novel synthetic SNIM.RNA technology based on uridine and cytidine replacement, resulting in an increased stability and lower immunogenicity of the produced mRNA.[56] In human HSPCs, a combination of MC-SB transposons with SNIM.RNA-SB100X supported the highest levels of transposition and persistent gene delivery (Figure 3).

Importantly, in addition to efficacy, the SB transposon system refined by combined implementation of MC DNA and SNIM.RNA technologies also offers several biosafety advantages over conventional plasmid DNA vectors. For the MC delivery platform in particular, the absence of bacterial plasmid backbone elements, such as antibiotic resistance gene and bacterial origin of replication, in therapeutic vectors is highly relevant in clinical application. Especially antibiotic resistance genes included in a therapeutic cell product and their possible uncontrolled dissemination in patient's bacterial flora by horizontal gene transfer following HSPC transplantation may raise safety concerns. In addition, the implementation of an mRNA source for transient delivery of transposase component of the SB system further increases the biosafety level of our approach, as mRNA does not bear the risk of chromosomal integration. In contrast, it is known that electroporation of plasmid DNA is associated with a small but non-negligible risk of spontaneous vector integration into the host genome.[69] Genomic integration of the SB100X-coding sequence into the HSPC genome represents a finite risk in a gene therapy application, because such event could lead to genomic instability due to prolonged and uncontrollable transposase expression, resulting in continuous remobilization of the already integrated SB transposon.

We addressed biosafety issues of SB-mediated stable gene delivery into HSPCs also by analyzing the integration profile of SB in CD34$^+$ cells. Consistent with the results obtained in other cell types,[9–13,70,71] the SB transposon system exhibits a close-to-random profile of genomic integration in HSPCs (Figure 6). No pronounced integration preferences could be observed with respect to genes and various intergenic regions, including TSSs. In contrast, γRV and lentiviral vectors commonly utilized in gene therapy tend to integrate in a non-random manner. Preferential integrations of γRV vectors near transcriptional regulatory elements of active genes[60,72,73] and of lentiviral vectors biased toward bodies of genes[73] are typically recovered, bearing an increased genotoxicity risk that already manifested in patients treated with γRV vectors by leukemogenesis during early gene therapy clinical trials.[2–5] The fairly random profile of SB integrations may offer a safer alternative for lifelong genetic correction of HSPCs.

For gene therapy to be effective it is necessary to (1) achieve robust delivery of the desired genes to the relevant target cells, (2) express the genes long term, and (3) minimize the risks of secondary effects. Non-viral SB transposon-based gene transfer may have certain advantages over viral vector systems, including limited immunogenicity, a characteristic random insertion profile, and economical production of Good Manufactoring Practice (GMP) vector batches for clinical use. However, non-viral gene transfer approaches typically result in pronounced cellular toxicity following transfection that limits stable gene transfer efficiencies in most primary cells. We demonstrated here a significant improvement in the efficiency of non-viral gene delivery into HSPCs by employing both MC DNA and SNIM.RNA technologies for intracellular delivery and activity of the SB transposon system. *Ex vivo* transfection of human CD34$^+$ cells with this enhanced transposon system yielded robust and stable gene expression, reaching up to 30%–40% of CD34$^+$ cells and CFUs (Figures 3 and 4).

Please cite this article in press as: Holstein et al., Efficient Non-viral Gene Delivery into Human Hematopoietic Stem Cells by Minicircle *Sleeping Beauty* Transposon Vectors, Molecular Therapy (2018), https://doi.org/10.1016/j.ymthe.2018.01.012

Our experiments involving the transplantation of nucleofected $CD34^+$ cells into immunodeficient mice (Figure 7) first showed that DNA nucleofection can mediate engraftment defects, consistent with previous observations.[16,74] Nevertheless, maintaining nucleofected cells in culture for 4–8 days limited graft failure and improved the engraftment of cells expressing the Venus marker gene. The results were most remarkable when $CD34^+$ cells were nucleofected with the Venus-MCs and the SB transposase as mRNA. Under these conditions, 6 of 6 transplanted mice showed high-level engraftment of $CD45^+$ cells, equivalent to those observed in mice transplanted with untreated cells. Moreover, in all these cases the presence of $Venus^+$ cells was evident. Because during these days in culture the number of non-integrated copies of nucleofected constructs is markedly reduced, our data suggest the convenience of infusing nucleofected cells after the dilution of unintegrated copies of the transposon vector system. Most significantly, our results unequivocally demonstrate that our optimized MC platforms mediate *in vivo* transgene expression both in the myeloid and lymphoid lineages, and even in primitive human hematopoietic $CD34^+$ cells in the bone marrow of transplanted mice, demonstrating efficient transposition in primitive hematopoietic repopulating cells. Taken together, we consider that this refined delivery platform of the SB transposon system constitutes a highly promising approach to be implemented for the clinical use of non-viral hematopoietic gene therapy.

MATERIALS AND METHODS

Generation and Production of SB Transposon and Transposase Minicircle DNA Constructs

In the present work, we utilized a ParA resolvase-based recombination system as an effective platform for large-scale and clinically relevant MC production.[39,75,76] The production of MC DNA is carried out in two major steps: the cultivation in a bioreactor and the purification by specific chromatographic steps. Cultivation of MC producer *E. coli* K12 cells was carried out at 37°C in a Sartorius-Stedim bioreactor BiostatC plus (Sartorius-Stedim, Guxhagen, Germany) with 10 or 20 L working volume used without addition of any antibiotics and grown in Luria-Bertani (LB) medium for approximately 15 hr. The recombinase expression was induced at an OD_{600} » 4 by adding L-arabinose. After 1 hr of further growth, cells were harvested by centrifugation, frozen, and DNA was purified, as described previously.[39,77] The recombination product (MC and mini-plasmid) was further purified after the primary recovery with a non-commercial proprietary affinity chromatography matrix[39] to specifically bind the MC and remove the other DNA molecules from the preparation. The specific binding of MC DNA was optimized with different ionic strength and pH values. The resulting MC was subject to multiple quality control tests to establish that the DNA was free of LPS-endotoxin, protein, RNA, and bacterial chromosomal DNA and that the MC was a homogeneous monomer (no multimers) in a supercoiled conformation.

Generation of SB Transposase in the Form of SNIM.RNA

The SB100X-coding sequences were excised from the expression plasmid pcGlobin2-SB100X[22] using *BamHI-EcoRI* and cloned into the respective sites of pVAXA120.[56] This vector is identical to pVAX1 (Invitrogen) with the exception of a stretch of 120 As between the PstI-*Not*I sites. Template DNA for the construct pVAXA120-SB100X was prepared using the Maxiprep kit from Macherey and Nagel. To generate template for *in vitro* transcription (IVT), pVAXA120-SB100X was linearized by restriction digestion using *Not*I. Linearized template plasmid DNA (pDNA) was further purified by chloroform ethanol sodium acetate purification. IVT was carried out using Ethris' proprietary IVT reaction mixture including T7 RNA polymerase, in which 25% of Cytidine-5′-Triphosphate and Uridine-5′-Triphosphate was replaced by 5-Methylcytidine-5′-Triphosphate and 2-Thiouridine-5′-Triphosphate (Jena Biosciences, Germany). Capping of the resulting cmRNA (chemically modified RNA) was performed using *Vaccinia* virus-capping enzyme and mRNA Cap 2′-O-Methyltransferase to generate a cap 1 structure. The mRNA was subsequently purified by ammonium acetate precipitation. Size and quality of the produced cmRNA was confirmed by Experion LabChip analysis.

Purification and Cultivation of $CD34^+$ Cells

The *in vitro* experiments shown in Figures 1, 2, 3, 4, 5, and 6 were done with $CD34^+$ cells isolated from apheresis products collected after peripheral blood stem cell mobilization induced by means of injections of granulocyte colony-stimulating factor. Apheresis products were obtained from three independent healthy donors after informed consent and with approval of the responsible Ethics Committee (Goethe University, Permit 329/10). Apheresis harvest was first subjected to red blood cell lysis using ACK Buffer (Invitrogen) and then to positive selection by magnetic cell separation using the MACS human CD34 MicroBead Kit, MACS separator, and MACS LS columns (Miltenyi Biotec), according to the manufacturer's instructions. Prior to nucleofection, $CD34^+$ cells were stimulated for 1.5–2.5 days in complete StemSpan serum-free medium (STEMCELL Technologies), which was supplemented with 2 mM L-glutamine and the following cytokine cocktail: 100 ng/mL human stem cell factor (hSCF), 100 ng/mL hFlt3-Ligand, and 100 ng/mL thrombopoietin (TPO) (PeproTech). Afterward, cell culture medium was gradually shifted to X-VIVO 20 (Lonza) supplemented with 2 mM L-glutamine and the same cytokine cocktail as described above. For long-term analysis, cells were maintained under standard cell culture conditions at a cell density of $0.5–1 \times 10^6$/mL until up to day 62 post-nucleofection.

The *in vivo* transplantation experiments shown in Figure 7 were done with cord blood-derived $CD34^+$ cells. Cord blood samples from healthy donors were obtained from the Madrid Community Transfusion Centre after informed consent of the mothers and under their institutional review board (IRB) approval and complying with the Helsinki Declaration. Mononuclear cells were purified by Ficoll-Paque PLUS (GE Healthcare, Fairfield, CT, USA) density gradient centrifugation, and $CD34^+$ magnetic-labeled cells were selected using CD34 MicroBead Kit.

Nucleofection of $CD34^+$ Cells

1×10^6 cells per sample were nucleofected with 10 μg SB transposon and 5 μg SB transposase construct, both provided either in plasmid

DNA or MC DNA form. In a mass-to-mass comparison, equal amounts of both MC SB vectors in relation to their plasmid counterparts were tested; in an equimolar comparison, the amount of both MC SB vectors was adjusted in order to provide the same numbers of vector particles as in the plasmid sample. Since one of our objectives was to reduce DNA amount-dependent nucleofection toxicity, no compensation with filler DNA was applied. In some control experiments, cells were nucleofected with 10 μg SB transposon alone or were subjected to nucleofection without DNA. In SNIM.RNA-based gene delivery experiments, the DNA vector carrying the SB100X transposase was replaced by 5 or 10 μg SNIM.RNA-SB. Cells were nucleofected using the 4D Nucleofector (Lonza) and E0100 program. After nucleofection, cells were resuspended in 2 mL complete StemSpan medium.

Flow Cytometry

Efficiency of transient and stable gene delivery was estimated by flow cytometry at days 2 and 15 post-nucleofection, respectively. Cell viability was determined at day 2 post-nucleofection. For that, around 1/10 of cell culture volume was collected, washed with PBS, and stained with DAPI/PBS solution. The cells were then subjected to flow cytometry using the BD LSR II Flow Cytometer (BD Biosciences). Gating for Venus signal was accomplished within the DAPI-negative cell population. The results were analyzed using the FCS Express 4 Flow Cytometry software (De Novo Software).

CFU Assay

Committed hematopoietic progenitors were quantified *in vitro* at day 2 post-nucleofection by seeding 4,000–4,500 purified $CD34^+$ cells/mL in methylcellulose medium MethoCult H4434 Classic (STEMCELL Technologies) enriched with a cytokine cocktail supporting the formation of BFU-E, CFU-E, CFU-GM, and CFU-GEMM. After 15 days of culture, hematopoietic colonies of different phenotypes were morphologically identified and counted using a Nikon Eclipse Ti-S microscope. Representative images of each type of cell colony were taken with a monochromatic camera using the 10× objective and the NIS Elements software (Nikon).

Transplants of NSG Mice

NSG mice were obtained from the Jackson Laboratory (Bar Harbor, ME, USA) and maintained at the CIEMAT animal facility (registration 28079-21 A). All experimental procedures were carried out according to European Directive 2010/63/UE on the use and protection of mammals used for experimentation and other scientific purposes. NSG mice were irradiated with 1.5 Gy 24 hr prior to transplantation. The 0.7–1 × 10^6 $CD34^+$ cells, or their equivalent cell products generated after cell expansion in complete StemSpan medium, were transplanted into NSG mice. Transplanted mice were culled at 3–4 months post-transplantation (mpt) and total bone marrow cells (BMCs) were analyzed by flow cytometry with hCD45 (304014, BioLegend), huCD19 (25-0198, eBioscience), hCD33 (A07775, Beckman Coulter), and hCD34 (555824, Becton Dickinson) monoclonal antibodies.

Real-Time PCR

Quantification of genomic VCN within the bulk cell population was performed by real-time PCR after 3 weeks of cell culture expansion. Genomic DNA (gDNA) was isolated using the DNeasy Blood & Tissue Kit (QIAGEN) according to the manufacturer's instructions. To exclude residual plasmid DNA from the DNA isolates, the samples were subjected to an overnight restriction digestion at 37°C using methylation-sensitive *Dpn*I restriction enzyme. The digest was then separated in an 0.8% agarose gel. The band representing the gDNA was cut out, and gDNA was purified with Zymoclean Large Fragment DNA Recovery Kit (Zymo Research). Real-time PCR was performed in triplicates using the KAPA SYBR FAST Universal kit (PeqLab) and the LightCycler (Roche). Genomic integrants of the SB transposon were detected using SB-IRDR-R_FW: 5′-GCTGAAATGAATCATTCTCTCTACTATTATTCTGA-3′ and SB-IRDR-R_RV: 5′-AATTCCCTGTCTTAGGTCAGTTAGGA-3′ primers. The gDNA content was normalized based on the amplification of the TERT gene using TERT_FW: 5′-GACAAAGTACAGCTCAGGCG-3′ and TERT_RV: 5′-TTCAGCGTGCTCAACTACGA-3′ primers. PCR conditions were as follows: 95°C for 10 min and 45 cycles of 95°C for 10 s, 60°C for 20 s, and 72°C for 10 s. The final VCN was determined using clonal gDNA standards carrying a defined number of genomic insertions of an SB transposon. Results were analyzed using the LightCycler 96 Software (Roche).

Droplet Digital PCR

Quantification of genomic VCN from cell colonies was performed by droplet digital PCR after at least 3 weeks of colony growth in methylcellulose medium. Individual colonies derived from 3 independent experiments were picked, and gDNA was isolated using the Quick-gDNA MicroPrep (Zymo Research). To exclude residual plasmid DNA from the gDNA amplification template, the obtained DNA fraction was subjected to an overnight digestion at 37°C using methylation-sensitive *Dpn*I restriction enzyme. Afterward, gDNA was fragmented by a 2-hr digestion at 25°C using CviQI restriction enzyme. Quantification of genomic VCN was performed using the QX100 Droplet Digital PCR System (Bio-Rad) and ddPCR Supermix for Probes (Bio-Rad). The SB integrants were detected by amplification of transposon's right inverted repeats (RIRs) using RIR_FW: 5′-GAATGTGATGAAAGAAATAAA-3′ and RIR_RV: 5′-AGTTTACATACACCTTAGCC-3′ primers and the RIR-specific probe: 5′-FAM-TGGTGATCCTAACTGACCTAAGACAGG-BH1-3′. The results were normalized based on the amplification of the RPP30 gene using RPP30_FW: 5′-GGTTAACTACAGCTCCCAGC-3′ and RPP30_RV: 5′-CTGTCTCCACAAGTCCGC-3′ primers. The 5′-HEX-TGGACCTGCGAGCGGGTTCTGACC-BH1-3′ probe served then for detection of RPP30 amplicons. PCR conditions were as follows: 95°C for 10 min; 40 cycles of 94°C for 10 s, 53°C for 20 s, and 60°C for 10 s; and 98°C for 10 min. The results were analyzed using the QuantaSoft software (Bio-Rad).

Insertion Site Library Preparation and Bioinformatic Analysis

The preparation of the Illumina sequencing-compatible insertion site libraries was described earlier.[13] Briefly, agarose gel-purified high molecular gDNA was sonicated to an average size of

Please cite this article in press as: Holstein et al., Efficient Non-viral Gene Delivery into Human Hematopoietic Stem Cells by Minicircle *Sleeping Beauty* Transposon Vectors, Molecular Therapy (2018), https://doi.org/10.1016/j.ymthe.2018.01.012

500 bp and ligated to custom linkers, and nested PCR reactions were used to generate multiplexed libraries containing the transposon ends and flanking genomic sequences for Illumina HiSeq sequencing. The conditions and thresholds of the raw read processing and mapping parameters have been specified previously.[13] In short, the raw reads were subjected to quality trimming, and the resulting reads were mapped to the hg19 human genome assembly with *bowtie*[78] in cycling mapping using the TAPDANCE algorithm.[79]

For the comparative analysis with SB integration profile, we used γRV and lentiviral insertion site datasets produced by linker-mediated PCR (LM-PCR) coupled to Roche-454 pyrosequencing from human cord blood-derived $CD34^+$ HSPCs, as previously described.[60] Additional lentiviral integration sites were obtained from the same cell sample by adapting the LM-PCR technique to Illumina MiSeq sequencing. Essentially, the nested primers were flanked by the following sequences: 5′-TCGTCGGCAGCGTCAGATGTGTATAAGAGACA-(viral LTR-nested primer) and 5′-GTCTCGTGGGCTCGGAGATGTGTATAAGAGACAG-linker-nested primer). MiSeq v3 reagents were used to sequence the LM-PCR library at saturation-producing paired-end 300-bp reads, following the standard operational instructions. Trimming of the sequencing reads was performed by *bowtie*,[78] and the sequence mapping onto the human reference genome (hg19 assembly) was performed as previously described.[60]

Genomic segmentation and whole-transcriptome RNA sequencing (RNA-seq) datasets for human HSPCs were obtained from the NIH Roadmap Epigenomics Mapping Consortium.[61] Analyses of the representation of the insertions in genomic regions of interest were done in R using the *genomation* package.[80] For the correlation of gene expression levels and insertion frequencies, reads per kilobase per million mapped reads (RPKM) values of all known, non-redundant human transcription units were used to group the genes to ten pools of equal size with increasing expression values. For the analysis of insertions in GSHs, the corresponding genomic coordinates were downloaded from the UCSC Genome Browser database (http://genome.ucsc.edu/cgi-bin/hgTables?command=start); for the genes implicated in cancer, we used the *AllOnco* collection.[63]

To measure the association of the vector insertions with active genes involved in known human disease phenotypes,[81] we selected all insertions within gene bodies and in segments up to 10 kb upstream of the TSSs of expressed protein-coding genes in human HSPCs. Genes were designated as transcriptionally active with RPKM values greater than or equal to the first quantile of the count range. Lists of these vector insertions were analyzed with the Genomic Regions Enrichment of Annotations Tool (GREAT) algorithm[82] using default settings. Associations with human phenotypes were considered statistically significant if both the binomial test over genomic regions and a hypergeometric test over genes resulted in false discovery rate (FDR) Q-values ≤ 0.05.

Statistical Analysis

For all statistical analyses, significance was set as $*0.01 \leq p \leq 0.05$ and $**0.001 \leq p \leq 0.01$ throughout the experiments. For correlation analysis, we performed a Pearson correlation after checking the Gaussian distribution of the sampled data using D'Agostino and Pearson, Shapiro-Wilk, and Kolmogorov-Smirnov normality tests. Two-tailed p value was computed in all cases.

SUPPLEMENTAL INFORMATION

Supplemental Information includes seven figures and can be found with this article online at https://doi.org/10.1016/j.ymthe.2018.01.012.

AUTHOR CONTRIBUTIONS

M.H. designed research, executed most of the experiments *in vitro*, analyzed the data, and wrote the paper. C.M.-N. executed most of the *in vivo* experiments and analyzed data. C.M. generated transposon insertion libraries and executed the bioinformatic analyses. E.A. contributed to the mouse transplantation work. V.P. delivered *de novo* lentiviral insertion datasets. M. Schmeer delivered the MCs. E.G. performed statistical analysis. J.C.O.F. performed copy number analysis with droplet digital PCR. D.K. and W.W. generated the transposon precursor plasmids for MC production. M.K.A. and J.G. generated vectors for mRNA production and delivered SNIM RNA. H.B.B. contributed $CD34^+$ cells for the study and wrote the paper. Z. Izsvák contributed to the design of transposon MCs. M. Schleef contributed the MCs for the study. C.R. contributed the SNIM RNA for the study. F.M. contributed retroviral and lentiviral datasets for the study and wrote the paper. J.A.B. and G.G. designed research, contributed the *in vivo* studies, analyzed the data, and wrote the paper. Z. Ivics supervised the project, designed research, analyzed the data, and wrote the paper.

CONFLICTS OF INTEREST

M.H., C.R., M. Schmeer, M. Schleef, and Z. Ivics are inventors on patent applications related to this work.

ACKNOWLEDGMENTS

This work was supported by the Center for Cell and Gene Therapy of the LOEWE (Landes-Offensive zur Entwicklung Wissenschaftlich-ökonomischer Exzellenz) program in Hessen, Germany, and by grants from the Deutsche Forschungsgemeinschaft (IV 21/11-1); the European Research Council (ERC-2010-AdG, GT-SKIN); the European Commission (H2020-PHC-2015-666908, SCIDNET); the Spanish Ministry of Economy, Industry and Competitiveness and FEDER (SAF2015-68073-R, FAMOCURE); and "Fondo de Investigaciones Sanitarias, Instituto de Salud Carlos III" (RD12/0019/0023). CIBERER is an initiative of the "Instituto de Salud Carlos III" and "Fondo Europeo de Desarrollo Regional (FEDER)." C.M.-N. was supported by a fellowship of the CIBERER (Spain).

REFERENCES

1. Booth, C., Gaspar, H.B., and Thrasher, A.J. (2016). Treating Immunodeficiency through HSC Gene Therapy. Trends Mol. Med. *22*, 317–327.

2. Hacein-Bey-Abina, S., Von Kalle, C., Schmidt, M., McCormack, M.P., Wulffraat, N., Leboulch, P., Lim, A., Osborne, C.S., Pawliuk, R., Morillon, E., et al. (2003). LMO2-associated clonal T cell proliferation in two patients after gene therapy for SCID-X1. Science *302*, 415–419.

3. Hacein-Bey-Abina, S., Garrigue, A., Wang, G.P., Soulier, J., Lim, A., Morillon, E., Clappier, E., Caccavelli, L., Delabesse, E., Beldjord, K., et al. (2008). Insertional oncogenesis in 4 patients after retrovirus-mediated gene therapy of SCID-X1. J. Clin. Invest. *118*, 3132–3142.

4. Ott, M.G., Schmidt, M., Schwarzwaelder, K., Stein, S., Siler, U., Koehl, U., Glimm, H., Kühlcke, K., Schilz, A., Kunkel, H., et al. (2006). Correction of X-linked chronic granulomatous disease by gene therapy, augmented by insertional activation of MDS1-EVI1, PRDM16 or SETBP1. Nat. Med. *12*, 401–409.

5. Howe, S.J., Mansour, M.R., Schwarzwaelder, K., Bartholomae, C., Hubank, M., Kempski, H., Brugman, M.H., Pike-Overzet, K., Chatters, S.J., de Ridder, D., et al. (2008). Insertional mutagenesis combined with acquired somatic mutations causes leukemogenesis following gene therapy of SCID-X1 patients. J. Clin. Invest. *118*, 3143–3150.

6. Naldini, L., Blömer, U., Gallay, P., Ory, D., Mulligan, R., Gage, F.H., Verma, I.M., and Trono, D. (1996). In vivo gene delivery and stable transduction of nondividing cells by a lentiviral vector. Science *272*, 263–267.

7. Bai, Y., Soda, Y., Izawa, K., Tanabe, T., Kang, X., Tojo, A., Hoshino, H., Miyoshi, H., Asano, S., and Tani, K. (2003). Effective transduction and stable transgene expression in human blood cells by a third-generation lentiviral vector. Gene Ther. *10*, 1446–1457.

8. Thornhill, S.I., Schambach, A., Howe, S.J., Ulaganathan, M., Grassman, E., Williams, D., Schiedlmeier, B., Sebire, N.J., Gaspar, H.B., Kinnon, C., et al. (2008). Self-inactivating gammaretroviral vectors for gene therapy of X-linked severe combined immunodeficiency. Mol. Ther. *16*, 590–598.

9. Vigdal, T.J., Kaufman, C.D., Izsvák, Z., Voytas, D.F., and Ivics, Z. (2002). Common physical properties of DNA affecting target site selection of sleeping beauty and other Tc1/mariner transposable elements. J. Mol. Biol. *323*, 441–452.

10. Huang, X., Guo, H., Tammana, S., Jung, Y.C., Mellgren, E., Bassi, P., Cao, Q., Tu, Z.J., Kim, Y.C., Ekker, S.C., et al. (2010). Gene transfer efficiency and genome-wide integration profiling of Sleeping Beauty, Tol2, and piggyBac transposons in human primary T cells. Mol. Ther. *18*, 1803–1813.

11. Yant, S.R., Wu, X., Huang, Y., Garrison, B., Burgess, S.M., and Kay, M.A. (2005). High-resolution genome-wide mapping of transposon integration in mammals. Mol. Cell. Biol. *25*, 2085–2094.

12. Gogol-Döring, A., Ammar, I., Gupta, S., Bunse, M., Miskey, C., Chen, W., Uckert, W., Schulz, T.F., Izsvák, Z., and Ivics, Z. (2016). Genome-wide Profiling Reveals Remarkable Parallels Between Insertion Site Selection Properties of the MLV Retrovirus and the piggyBac Transposon in Primary Human CD4(+) T Cells. Mol. Ther. *24*, 592–606.

13. Monjezi, R., Miskey, C., Gogishvili, T., Schleef, M., Schmeer, M., Einsele, H., Ivics, Z., and Hudecek, M. (2017). Enhanced CAR T-cell engineering using non-viral Sleeping Beauty transposition from minicircle vectors. Leukemia *31*, 186–194.

14. Walisko, O., Schorn, A., Rolfs, F., Devaraj, A., Miskey, C., Izsvák, Z., and Ivics, Z. (2008). Transcriptional activities of the Sleeping Beauty transposon and shielding its genetic cargo with insulators. Mol. Ther. *16*, 359–369.

15. Ivics, Z., Hackett, P.B., Plasterk, R.H., and Izsvák, Z. (1997). Molecular reconstruction of Sleeping Beauty, a Tc1-like transposon from fish, and its transposition in human cells. Cell *91*, 501–510.

16. Mátés, L., Chuah, M.K., Belay, E., Jerchow, B., Manoj, N., Acosta-Sanchez, A., Grzela, D.P., Schmitt, A., Becker, K., Matrai, J., et al. (2009). Molecular evolution of a novel hyperactive Sleeping Beauty transposase enables robust stable gene transfer in vertebrates. Nat. Genet. *41*, 753–761.

17. Ivics, Z., Li, M.A., Mátés, L., Boeke, J.D., Nagy, A., Bradley, A., and Izsvák, Z. (2009). Transposon-mediated genome manipulation in vertebrates. Nat. Methods *6*, 415–422.

18. Copeland, N.G., and Jenkins, N.A. (2010). Harnessing transposons for cancer gene discovery. Nat. Rev. Cancer *10*, 696–706.

19. DeNicola, G.M., Karreth, F.A., Adams, D.J., and Wong, C.C. (2015). The utility of transposon mutagenesis for cancer studies in the era of genome editing. Genome Biol. *16*, 229.

20. Ivics, Z., Garrels, W., Mátés, L., Yau, T.Y., Bashir, S., Zidek, V., Landa, V., Geurts, A., Pravenec, M., Rülicke, T., et al. (2014). Germline transgenesis in pigs by cytoplasmic microinjection of Sleeping Beauty transposons. Nat. Protoc. *9*, 810–827.

21. Ivics, Z., Hiripi, L., Hoffmann, O.I., Mátés, L., Yau, T.Y., Bashir, S., Zidek, V., Landa, V., Geurts, A., Pravenec, M., et al. (2014). Germline transgenesis in rabbits by pronuclear microinjection of Sleeping Beauty transposons. Nat. Protoc. *9*, 794–809.

22. Ivics, Z., Mátés, L., Yau, T.Y., Landa, V., Zidek, V., Bashir, S., Hoffmann, O.I., Hiripi, L., Garrels, W., Kues, W.A., et al. (2014). Germline transgenesis in rodents by pronuclear microinjection of Sleeping Beauty transposons. Nat. Protoc. *9*, 773–793.

23. Izsvák, Z., Hackett, P.B., Cooper, L.J., and Ivics, Z. (2010). Translating Sleeping Beauty transposition into cellular therapies: victories and challenges. BioEssays *32*, 756–767.

24. Ivics, Z., and Izsvák, Z. (2010). The expanding universe of transposon technologies for gene and cell engineering. Mob. DNA *1*, 25.

25. Ivics, Z., and Izsvák, Z. (2011). Nonviral gene delivery with the sleeping beauty transposon system. Hum. Gene Ther. *22*, 1043–1051.

26. Swierczek, M., Izsvák, Z., and Ivics, Z. (2012). The Sleeping Beauty transposon system for clinical applications. Expert Opin. Biol. Ther. *12*, 139–153.

27. Williams, D.A. (2008). Sleeping beauty vector system moves toward human trials in the United States. Mol. Ther. *16*, 1515–1516.

28. Singh, H., Figliola, M.J., Dawson, M.J., Olivares, S., Zhang, L., Yang, G., Maiti, S., Manuri, P., Senyukov, V., Jena, B., et al. (2013). Manufacture of clinical-grade CD19-specific T cells stably expressing chimeric antigen receptor using Sleeping Beauty system and artificial antigen presenting cells. PLoS ONE *8*, e64138.

29. Singh, H., Huls, H., Kebriaei, P., and Cooper, L.J.N. (2014). A new approach to gene therapy using Sleeping Beauty to genetically modify clinical-grade T cells to target CD19. Immunol. Rev. *257*, 181–190.

30. Kebriaei, P., Singh, H., Huls, M.H., Figliola, M.J., Bassett, R., Olivares, S., Jena, B., Dawson, M.J., Kumaresan, P.R., Su, S., et al. (2016). Phase I trials using Sleeping Beauty to generate CD19-specific CAR T cells. J. Clin. Invest. *126*, 3363–3376.

31. Xue, X., Huang, X., Nodland, S.E., Mátés, L., Ma, L., Izsvák, Z., Ivics, Z., LeBien, T.W., McIvor, R.S., Wagner, J.E., and Zhou, X. (2009). Stable gene transfer and expression in cord blood-derived CD34+ hematopoietic stem and progenitor cells by a hyperactive Sleeping Beauty transposon system. Blood *114*, 1319–1330.

32. Hamm, A., Krott, N., Breibach, I., Blindt, R., and Bosserhoff, A.K. (2002). Efficient transfection method for primary cells. Tissue Eng. *8*, 235–245.

33. Gresch, O., Engel, F.B., Nesic, D., Tran, T.T., England, H.M., Hickman, E.S., Körner, I., Gan, L., Chen, S., Castro-Obregon, S., et al. (2004). New non-viral method for gene transfer into primary cells. Methods *33*, 151–163.

34. von Levetzow, G., Spanholtz, J., Beckmann, J., Fischer, J., Kögler, G., Wernet, P., Punzel, M., and Giebel, B. (2006). Nucleofection, an efficient nonviral method to transfer genes into human hematopoietic stem and progenitor cells. Stem Cells Dev. *15*, 278–285.

35. Hemmi, H., Takeuchi, O., Kawai, T., Kaisho, T., Sato, S., Sanjo, H., Matsumoto, M., Hoshino, K., Wagner, H., Takeda, K., and Akira, S. (2000). A Toll-like receptor recognizes bacterial DNA. Nature *408*, 740–745.

36. Chuang, T.-H., Lee, J., Kline, L., Mathison, J.C., and Ulevitch, R.J. (2002). Toll-like receptor 9 mediates CpG-DNA signaling. J. Leukoc. Biol. *71*, 538–544.

37. Huerfano, S., Ryabchenko, B., and Forstová, J. (2013). Nucleofection of expression vectors induces a robust interferon response and inhibition of cell proliferation. DNA Cell Biol. *32*, 467–479.

38. Darquet, A.M., Cameron, B., Wils, P., Scherman, D., and Crouzet, J. (1997). A new DNA vehicle for nonviral gene delivery: supercoiled minicircle. Gene Ther. *4*, 1341–1349.

39. Mayrhofer, P., Blaesen, M., Schleef, M., and Jechlinger, W. (2008). Minicircle-DNA production by site specific recombination and protein-DNA interaction chromatography. J. Gene Med. *10*, 1253–1269.

40. Bigger, B.W., Tolmachov, O., Collombet, J.M., Fragkos, M., Palaszewski, I., and Coutelle, C. (2001). An araC-controlled bacterial cre expression system to produce DNA minicircle vectors for nuclear and mitochondrial gene therapy. J. Biol. Chem. *276*, 23018–23027.

41. Chabot, S., Orio, J., Schmeer, M., Schleef, M., Golzio, M., and Teissié, J. (2013). Minicircle DNA electrotransfer for efficient tissue-targeted gene delivery. Gene Ther. *20*, 62–68.

42. Kobelt, D., Schleef, M., Schmeer, M., Aumann, J., Schlag, P.M., and Walther, W. (2013). Performance of high quality minicircle DNA for in vitro and in vivo gene transfer. Mol. Biotechnol. *53*, 80–89.

43. Chen, Z.-Y., He, C.-Y., Ehrhardt, A., and Kay, M.A. (2003). Minicircle DNA vectors devoid of bacterial DNA result in persistent and high-level transgene expression in vivo. Mol. Ther. *8*, 495–500.

44. Osborn, M.J., McElmurry, R.T., Lees, C.J., DeFeo, A.P., Chen, Z.Y., Kay, M.A., Naldini, L., Freeman, G., Tolar, J., and Blazar, B.R. (2011). Minicircle DNA-based gene therapy coupled with immune modulation permits long-term expression of α-L-iduronidase in mice with mucopolysaccharidosis type I. Mol. Ther. *19*, 450–460.

45. Vaysse, L., Gregory, L.G., Harbottle, R.P., Perouzel, E., Tolmachov, O., and Coutelle, C. (2006). Nuclear-targeted minicircle to enhance gene transfer with non-viral vectors in vitro and in vivo. J. Gene Med. *8*, 754–763.

46. Darquet, A.M., Rangara, R., Kreiss, P., Schwartz, B., Naimi, S., Delaère, P., Crouzet, J., and Scherman, D. (1999). Minicircle: an improved DNA molecule for in vitro and in vivo gene transfer. Gene Ther. *6*, 209–218.

47. Dad, A.-B., Ramakrishna, S., Song, M., and Kim, H. (2014). Enhanced gene disruption by programmable nucleases delivered by a minicircle vector. Gene Ther. *21*, 921–930.

48. Jia, F., Wilson, K.D., Sun, N., Gupta, D.M., Huang, M., Li, Z., Panetta, N.J., Chen, Z.Y., Robbins, R.C., Kay, M.A., et al. (2010). A nonviral minicircle vector for deriving human iPS cells. Nat. Methods *7*, 197–199.

49. Wang, Q., Jiang, W., Chen, Y., Liu, P., Sheng, C., Chen, S., Zhang, H., Pan, C., Gao, S., and Huang, W. (2014). In vivo electroporation of minicircle DNA as a novel method of vaccine delivery to enhance HIV-1-specific immune responses. J. Virol. *88*, 1924–1934.

50. Ronald, J.A., Chuang, H.-Y., Dragulescu-Andrasi, A., Hori, S.S., and Gambhir, S.S. (2015). Detecting cancers through tumor-activatable minicircles that lead to a detectable blood biomarker. Proc. Natl. Acad. Sci. USA *112*, 3068–3073.

51. Hou, X., Jiao, R., Guo, X., Wang, T., Chen, P., Wang, D., Chen, Y., He, C.Y., and Chen, Z.Y. (2016). Construction of minicircle DNA vectors capable of correcting familial hypercholesterolemia phenotype in a LDLR-deficient mouse model. Gene Ther. *23*, 657–663.

52. Sharma, N., Cai, Y., Bak, R.O., Jakobsen, M.R., Schrøder, L.D., and Mikkelsen, J.G. (2013). Efficient sleeping beauty DNA transposition from DNA minicircles. Mol. Ther. Nucleic Acids *2*, e74.

53. Wiehe, J.M., Ponsaerts, P., Rojewski, M.T., Homann, J.M., Greiner, J., Kronawitter, D., Schrezenmeier, H., Hombach, V., Wiesneth, M., Zimmermann, O., and Torzewski, J. (2007). mRNA-mediated gene delivery into human progenitor cells promotes highly efficient protein expression. J. Cell. Mol. Med. *11*, 521–530.

54. Wilber, A., Frandsen, J.L., Geurts, J.L., Largaespada, D.A., Hackett, P.B., and McIvor, R.S. (2006). RNA as a source of transposase for Sleeping Beauty-mediated gene insertion and expression in somatic cells and tissues. Mol. Ther. *13*, 625–630.

55. Wilber, A., Wangensteen, K.J., Chen, Y., Zhuo, L., Frandsen, J.L., Bell, J.B., Chen, Z.J., Ekker, S.C., McIvor, R.S., and Wang, X. (2007). Messenger RNA as a source of transposase for sleeping beauty transposon-mediated correction of hereditary tyrosinemia type I. Mol. Ther. *15*, 1280–1287.

56. Kormann, M.S.D., Hasenpusch, G., Aneja, M.K., Nica, G., Flemmer, A.W., Herber-Jonat, S., Huppmann, M., Mays, L.E., Illenyi, M., Schams, A., et al. (2011). Expression of therapeutic proteins after delivery of chemically modified mRNA in mice. Nat. Biotechnol. *29*, 154–157.

57. Hu, J., Cutrera, J., and Li, S. (2014). The impact of non-electrical factors on electrical gene transfer. Methods Mol. Biol. *1121*, 47–54.

58. Maucksch, C., Bohla, A., Hoffmann, F., Schleef, M., Aneja, M.K., Elfinger, M., Hartl, D., and Rudolph, C. (2009). Transgene expression of transfected supercoiled plasmid DNA concatemers in mammalian cells. J. Gene Med. *11*, 444–453.

59. Lechardeur, D., Sohn, K.J., Haardt, M., Joshi, P.B., Monck, M., Graham, R.W., Beatty, B., Squire, J., O'Brodovich, H., and Lukacs, G.L. (1999). Metabolic instability of plasmid DNA in the cytosol: a potential barrier to gene transfer. Gene Ther. *6*, 482–497.

60. Cattoglio, C., Pellin, D., Rizzi, E., Maruggi, G., Corti, G., Miselli, F., Sartori, D., Guffanti, A., Di Serio, C., Ambrosi, A., et al. (2010). High-definition mapping of retroviral integration sites identifies active regulatory elements in human multipotent hematopoietic progenitors. Blood *116*, 5507–5517.

61. Kundaje, A., Meuleman, W., Ernst, J., Bilenky, M., Yen, A., Heravi-Moussavi, A., Kheradpour, P., Zhang, Z., Wang, J., Ziller, M.J., et al.; Roadmap Epigenomics Consortium (2015). Integrative analysis of 111 reference human epigenomes. Nature *518*, 317–330.

62. Papapetrou, E.P., Lee, G., Malani, N., Setty, M., Riviere, I., Tirunagari, L.M., Kadota, K., Roth, S.L., Giardina, P., Viale, A., et al. (2011). Genomic safe harbors permit high β-globin transgene expression in thalassemia induced pluripotent stem cells. Nat. Biotechnol. *29*, 73–78.

63. Sadelain, M., Papapetrou, E.P., and Bushman, F.D. (2011). Safe harbours for the integration of new DNA in the human genome. Nat. Rev. Cancer *12*, 51–58.

64. Hyde, S.C., Pringle, I.A., Abdullah, S., Lawton, A.E., Davies, L.A., Varathalingam, A., Nunez-Alonso, G., Green, A.M., Bazzani, R.P., Sumner-Jones, S.G., et al. (2008). CpG-free plasmids confer reduced inflammation and sustained pulmonary gene expression. Nat. Biotechnol. *26*, 549–551.

65. Reyes-Sandoval, A., and Ertl, H.C.J. (2004). CpG methylation of a plasmid vector results in extended transgene product expression by circumventing induction of immune responses. Mol. Ther. *9*, 249–261.

66. Chen, Z.Y., He, C.Y., Meuse, L., and Kay, M.A. (2004). Silencing of episomal transgene expression by plasmid bacterial DNA elements in vivo. Gene Ther. *11*, 856–864.

67. Chen, Z.-Y., Riu, E., He, C.-Y., Xu, H., and Kay, M.A. (2008). Silencing of episomal transgene expression in liver by plasmid bacterial backbone DNA is independent of CpG methylation. Mol. Ther. *16*, 548–556.

68. Izsvák, Z., Ivics, Z., and Plasterk, R.H. (2000). Sleeping Beauty, a wide host-range transposon vector for genetic transformation in vertebrates. J. Mol. Biol. *302*, 93–102.

69. Wang, Z., Troilo, P.J., Wang, X., Griffiths, T.G., Pacchione, S.J., Barnum, A.B., Harper, L.B., Pauley, C.J., Niu, Z., Denisova, L., et al. (2004). Detection of integration of plasmid DNA into host genomic DNA following intramuscular injection and electroporation. Gene Ther. *11*, 711–721.

70. Ammar, I., Gogol-Döring, A., Miskey, C., Chen, W., Cathomen, T., Izsvák, Z., and Ivics, Z. (2012). Retargeting transposon insertions by the adeno-associated virus Rep protein. Nucleic Acids Res. *40*, 6693–6712.

71. Voigt, K., Gogol-Döring, A., Miskey, C., Chen, W., Cathomen, T., Izsvák, Z., and Ivics, Z. (2012). Retargeting sleeping beauty transposon insertions by engineered zinc finger DNA-binding domains. Mol. Ther. *20*, 1852–1862.

72. De Ravin, S.S., Su, L., Theobald, N., Choi, U., Macpherson, J.L., Poidinger, M., Symonds, G., Pond, S.M., Ferris, A.L., Hughes, S.H., et al. (2014). Enhancers are major targets for murine leukemia virus vector integration. J. Virol. *88*, 4504–4513.

73. Cavazza, A., Moiani, A., and Mavilio, F. (2013). Mechanisms of retroviral integration and mutagenesis. Hum. Gene Ther. *24*, 119–131.

74. Hollis, R.P., Nightingale, S.J., Wang, X., Pepper, K.A., Yu, X.J., Barsky, L., Crooks, G.M., and Kohn, D.B. (2006). Stable gene transfer to human CD34(+) hematopoietic cells using the Sleeping Beauty transposon. Exp. Hematol. *34*, 1333–1343.

75. Jechlinger, W., Azimpour Tabrizi, C., Lubitz, W., and Mayrhofer, P. (2004). Minicircle DNA immobilized in bacterial ghosts: in vivo production of safe non-viral DNA delivery vehicles. J. Mol. Microbiol. Biotechnol. *8*, 222–231.

76. Mayrhofer, P., Schleef, M., and Jechlinger, W. (2009). Use of minicircle plasmids for gene therapy. Methods Mol. Biol. *542*, 87–104.

77. Rischmüller, A., Viefhues, M., Dieding, M., Blaesen, M., Schmeer, M., Baier, R., Anselmetti, D., and Schleef, M. (2013). Analytical tools in minicircle production. In Minicircle and Miniplasmid DNA Vectors: The Future of Non-Viral and Viral Gene Transfer, M. Schleef, ed. (Wiley-VCH Verlag GmbH & Co. KGaA), pp. 71–91.

78. Langmead, B., Trapnell, C., Pop, M., and Salzberg, S.L. (2009). Ultrafast and memory-efficient alignment of short DNA sequences to the human genome. Genome Biol. *10*, R25.

79. Sarver, A.L., Erdman, J., Starr, T., Largaespada, D.A., and Silverstein, K.A. (2012). TAPDANCE: an automated tool to identify and annotate transposon insertion CISs and associations between CISs from next generation sequence data. BMC Bioinformatics *13*, 154.

80. Akalin, A., Franke, V., Vlahoviček, K., Mason, C.E., and Schübeler, D. (2015). Genomation: a toolkit to summarize, annotate and visualize genomic intervals. Bioinformatics *31*, 1127–1129.

81. Robinson, P.N., and Mundlos, S. (2010). The human phenotype ontology. Clin. Genet. *77*, 525–534.

82. McLean, C.Y., Bristor, D., Hiller, M., Clarke, S.L., Schaar, B.T., Lowe, C.B., Wenger, A.M., and Bejerano, G. (2010). GREAT improves functional interpretation of cis-regulatory regions. Nat. Biotechnol. *28*, 495–501.